AD-A131 302 NEUROCOGNITIVE PATTERN ANALYSIS(U) EEG SYSTEMS LAB SAN FRANCISCO CA A S GEVINS ET AL. AUG 83 ONR-83-AE N00014-83-C-0022 1/1

UNCLASSIFIED F/G 5/10 NL

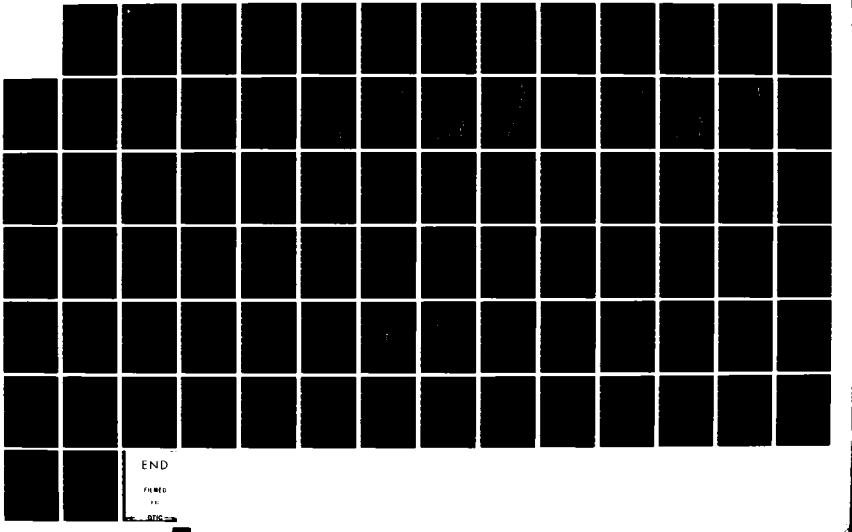

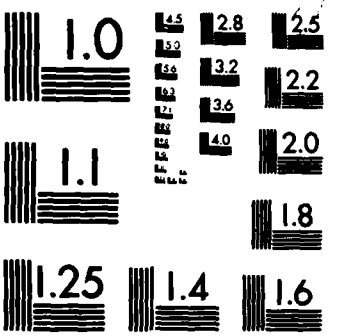

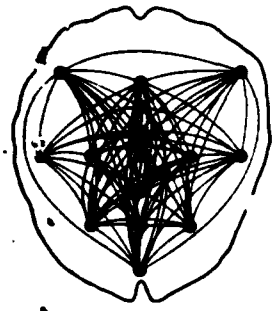

EEG SYSTEMS LABORATORY

1855 FOLSOM ST.
SAN FRANCISCO CA 94103
(415) 621-8343

Item 003AE

1 AUG 83

ANNUAL TECHNICAL REPORT

(ONR Contract Number N00014-83-C-0022)

1 NOV 82 -- 31 OCT 83

NEUROCOGNITIVE PATTERN ANALYSIS

D. Woodward, Scientific Officer
Life Sciences Directorate
Office of Naval Research
800 North Quincy Street
Arlington, VA 22217

A. Gevins, Director

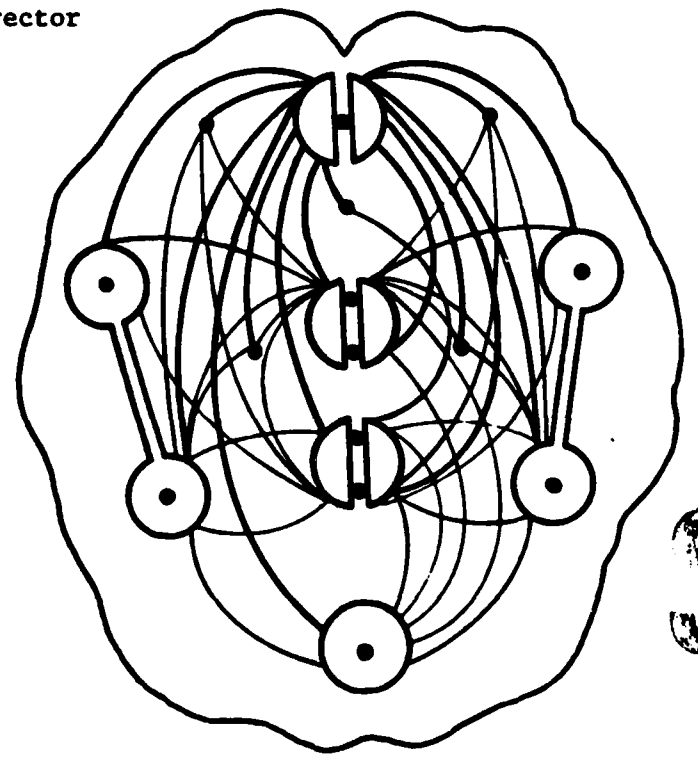

83 08 08 115

Unclassified

SECURITY CLASSIFICATION OF THIS PAGE (When Data Entered)

REPORT DOCUMENTATION PAGE		READ INSTRUCTIONS BEFORE COMPLETING FORM
1. REPORT NUMBER: ONR 83-AE	2. GOVT ACCESSION NO.: AD-A131302	3. RECIPIENT'S CATALOG NUMBER:
4. TITLE (and Subtitle): NEUROCOGNITIVE PATTERN ANALYSIS		5. TYPE OF REPORT & PERIOD COVERED: Final Report 1 NOV 82 to 31 OCT 83
		6. PERFORMING ORG. REPORT NUMBER:
7. AUTHOR(s): Alan S. Gevins, Brian A. Cutillo, Steven L. Bressler, Joseph C. Doyle, Robert S. Tannehill, & Gerald M. Zeitlin, Benjamin H. Bonham		8. CONTRACT OR GRANT NUMBER(s): N00014-82-C-0022
9. PERFORMING ORGANIZATION NAME AND ADDRESS: EEG Systems Laboratory 1855 Folsom San Francisco CA 94103		10. PROGRAM ELEMENT, PROJECT, TASK AREA & WORK UNIT NUMBERS:
11. CONTROLLING OFFICE NAME AND ADDRESS: Dr. Donald Woodward, Code 440 ONR, Life Sciences Directorate 800 North Quincy St. Arlington VA 22217		12. REPORT DATE: AUG 1983
		13. NUMBER OF PAGES: 80
14. MONITORING AGENCY NAME & ADDRESS (if different from Controlling Office)		15. SECURITY CLASS. (of this report): unclassified
		15a. DECLASSIFICATION/DOWNGRADING SCHEDULE:

16. DISTRIBUTION STATEMENT (of this Report)

Approved for public release; distribution unlimited

17. DISTRIBUTION STATEMENT (of the abstract entered in Block 20, if different from Report)

18. SUPPLEMENTARY NOTES

19. KEY WORDS (Continue on reverse side if necessary and identify by block number)

perceptuomotor, brain potentials, event related potentials, evoked correlations, single trial, digital signal processing, mathematical pattern recognition, neurocognitive, bimanual, artifact elimination.

20. ABSTRACT (Continue on reverse side if necessary and identify by block number)

Completed and ongoing studies of neurocognitive processes using the new technique of Neurocognitive Pattern (NCP) Analysis are reported. The pilot and formal recording phases of a bimanual visuomotor experiment are described, as well as work on the elimination of scalp-muscle and eye-movement artifacts from single-trial brain-potential data.

DD FORM 1 JAN 73 1473 EDITION OF 1 NOV 65 IS OBSOLETE

Unclassified

SECURITY CLASSIFICATION OF THIS PAGE (When Data Entered)

August 2, 1983 (34)(06)

I. OVERVIEW

A. Senior Scientific Personnel of the EEG Systems Laboratory

Benjamin H. Bonham, Electrical Engineer
Steven L. Bressler, Neurophysiologist
Brian A. Cutillo, Cognitive Scientist
Joseph C. Doyle, Neurophysicist
Alan S. Gevins, Director
Robert S. Tannehill, Programmer
Gerald M. Zeitlin, Systems Engineer

B. 1983 Papers

1. Gevins, A.S., Schaffer, R.E., Doyle, J.C., Cutillo, B.A., Tannehill, R.L. and Bressler, S.L. Shadows of thoughts: Rapidly changing, asymmetric, brain potential patterns of a brief visuomotor task. Science, 1983, 220, 97-99.

2. Gevins, A.S. Brain potentials and mental functions: methodological requirements. In I. Alter (Ed.), The Limits of Functional Localization, Raven Press, 1983, In press.

3. Gevins, A.S. Brain potential evidence for lateralization of higher cognitive functions. In J.B. Hellige (ed.), Cerebral Hemisphere Asymmetry: Method, Theory and Application, Praeger Press, 1983, 335-382.

4. Gevins, A.S. Brain Potentials and Human Higher Cognitive Functions: Methods, research and future directions. In J. H. Hannay (Ed.), Handbook of Neuropsychology. Oxford Press, 1983, In press.

C. Major Presentations, 1982-1983, A. Gevins

1. Symposium Chairman, American Association for the Advancement of Science, Washington, D.C., 1982.

2. Symposium Chairman, Winter Conference on Brain Research, Steamboat Springs, 1982.

3. Special Invited Lecturer, Int. Conf. Neuropsychology, Pittsburg, 1982.

4. Invited Speaker, Society for Biological Psychiatry, New York, 1983.

5. Symposium Chairman, IEEE Computer Design, New York, 1983.

6. Invited Lecturer, Third European EEG Conference, Basle, 1983.

7. Invited Lecturer, American EEG Society, New Orleans, 1983.

D. Experiments

The EEGSL is in the process of developing the method of Neurocognitive Pattern (NCP) Analysis for measuring aspects of mass neural processes related to perceptuomotor and cognitive activities. Several generations of NCP Analysis have been used to study both complex and simple tasks, and a number of findings have emerged. Taken together, these results suggest that neither strictly localizationist nor equipotentialist views of neurocognitive functioning are realistic. Since even simple tasks are associated with a rapidly shifting mosaic of focal scalp-recorded patterns, neurocognitive functioning might be better modeled as a network in which the activity of many specialized local processing elements is periodically integrated. Our research is directed toward developing methods for measuring these processes more precisely and modeling them more explicitly.

N.B. It must be understood that scalp-recorded potentials, even unaveraged timeseries, are not necessarily cortical in origin. Until this issue is settled, it is essential not to interpret scalp designations, which conventionally refer to underlying cortical areas, as implying measurement of the activity of cortical sources. For convenience, we use the conventional scalp designations subject to this caveat.

Specific findings include:

1. Complex perceptuomotor and cognitive activities such as reading and writing have unique, spatially differentiated scalp EEG spectral patterns. These patterns had sufficient specificity to identify the type of task from the EEG (EEG Clin. Neurophysiol. 47:693-703, 1979). The results were in accord with previous reports of hemispheric lateralization of 'spatial' and 'linguistic' processing.

2. When tasks are controlled for stimulus, response and performance-related factors, complex cognitive activities such as arithmetic, letter substitution and mental block rotation have identical, spatially diffuse EEG spectral scalp distributions. Compared with staring at a dot, such tasks had approximately 10% reductions in alpha and beta band spectral intensities (EEG Clin. Neurophysiol. 47: 704-710, 1979; Science 203:665-668, 1979). This reduction may be an index of their task workload. Since no patterns of hemispheric lateralization were found, this study suggested that previous reports of EEG hemispheric lateralization may have confounded EEG patterns related to limb and eye movements and arousal with those of mental activity per se (Science 207:1005-1008, 1980).

3. Split-second visuomotor tasks, controlled so that only the type of judgment varied, are associated with complex, rapidly shifting patterns of single-trial, evoked inter-electrode correlation of brain potential timeseries. Differences between spatial and numeric

judgments were evident in the task-cued prestimulus interval. Complex and often lateralized patterns of difference shifted with split-second rapidity from stimulus onset to just prior to response, at which time there was no difference between spatial and numeric tasks (Science 213:918-922, 1981). This suggested that once task-specific differential perceptual and cognitive processing was completed, a motor program common to both tasks was executed, regardless of differences in the stimuli or type of judgment.

4. Rapidly shifting, focal brain potential patterns, representing the maximal difference between similar split-second tasks, can be extracted with NCP Analysis. The move and no-move variants of a split-second visuospatial judgment task, which differed slightly in expectation, differed in type of judgment, and differed greatly in response, were associated with distinct differences in the patterns of single-trial evoked correlation between scalp-recorded channels (Science 220:97-99, 1983; see Sections III and IV). These patterns of difference increased in magnitude in each successive analysis interval. In the prestimulus interval, correlations of the midline frontal electrode distinguished the tasks ($p<.01$). In the interval spanning the N1, P2 and N2 event-related potential (ERP) peaks, the between-task evoked correlation contrast was focused at the midline parietal electrode ($p<.001$). In the interval centered on the P3a ERP peak, the focus of correlation difference was at the right parietal electrode and involved higher correlation of the right parietal with occipital and midline precentral electrodes in the no-move task, and with the right central electrode in the move task ($p<5 \times 10^{-5}$). In an interval centered 135 msec after the P3a ERP peak, which included right-handed response preparation and initiation, the focus of contrast shifted to the left central electrode, involving higher correlation with midline frontal and occipital electrodes in the move task and with the midline parietal electrode in the no-move task ($p<5 \times 10^{-6}$). These results concur with neuropsychological models of these tasks derived from clinical observations. They suggest that although simple perceptuomotor tasks are associated with a complex, dynamic mosaic of brain electrical patterns, it is possible to isolate foci of maximal differences between tasks. It is clear that without a split-second temporal resolution it is not possible to isolate the rapid shift in lateralization which presumably is associated with perceptual-cognitive and efferent processing stages.

5. The focal patterns of evoked correlation derived by NCP Analysis significantly distinguished the single-trial data of 7 of the 9 people in the above study. This suggested that similar neurocognitive mechanisms were being measured across the majority of participants (see Section IV).

6. Behaviorally identical trials of the move and no-move visuospatial tasks in the above study were found to be associated with distinctly different brain potential patterns (Section V). This suggests that appropriate brain potential measures may provide a tool for more detailed examination of previously unmeasured neurocognitive processes.

E. Analytic Methods

Neurocognitive Pattern (NCP) Analysis currently consists of the application of an adaptive-network, nonlinear mathematical pattern classification algorithm to extract task-related signals from sets of data. The analysis is applied to single-trial timeseries in brief time windows (100 to 175 msec) for up to 49 scalp electrodes. The data windows are determined for each person from the peaks of their averaged ERPs as well as from stimulus and response times, but measures are made on single trials.

1. Similarities and Differences Between NCP Analysis and Conventional ERP Analysis

NCP Analysis is grounded on the vast body of information gained from ERP methods and has the same underlying goal, namely to resolve spatially and temporally overlapping, task-related mass neural processes. However, it departs in several ways from the currently popular approach of extracting independent features from averaged ERPs by principal components analysis (PCA) followed by hypothesis testing with ANOVA. First, NCP Analysis is concerned with spatiotemporal task-related activity recorded by many electrodes in a number of time intervals from before the stimulus through the response. It quantifies neurocognitive activity in terms of a variety of parameters, rather than amplitude and latency of ERP components. Thus, it is possible that the increased dimensionality of parametrization may facilitate the measurement of subtler aspects of neurocognitive processes. Second, the questionable assumption of a multivariate normal distribution of brain potentials is not made in NCP Analysis. Third, brain-potential feature extraction and hypothesis testing are performed as a single process which determines features which are maximally different between the conditions of an experiment, rather than those which meet possibly irrelevant criteria such as statistical independence. Fourth, task-related patterns of consistency are extracted from sets of single-trial data. Significant results may be obtained as long as there is a pattern of consistent difference between tasks, even though the means of the two data sets do not differ significantly.

Taken together, these aspects of NCP Analysis may enable it to resolve small task-related signals from the obscuring background "noise" of the brain, revealing useful spatiotemporal information about mass neural processes. However, this is not without its costs. NCP Analysis requires several orders of magnitude more computing than PCA and ANOVA, and larger data sets than conventional ERP studies. Also, because of its sensitivity, highly controlled experimental paradigms are required to assure that the results are truly related to the hypothesis and not to spurious or idiosyncratic factors. (The process of developing one such task is described in Section II of this report.) This requires a greater allocation of effort and resources to experimental design, recording and analysis than is needed for most ERP experiments.

Although we have obtained several promising results with NCP Analysis,

the latest of which is described in Sections III and IV, we must caution that "the jury is still out". Additional basic studies are needed to determine whether NCP Analysis is really worthwhile. If so, it should be possible to optimize, standardize and simplify it for use in other laboratories.

2. Evoked Correlations Between Scalp Electrodes

For the past few years we have concentrated on a measure of the degree of waveshape similarity (crosscorrelation) between timeseries from pairs of electrodes. Measures of single channel power are also being used and preliminary results were described in last year's Final Report. The crosscorrelation approach is based on the (unproven) hypothesis that when areas of the brain are functionally related there is a consistent pattern of waveshape similarity between them. There are a number of considerations in interpreting the correlation patterns of scalp recordings, such as volume conduction from subcortical sources and driving by distant sources. Some of the ambiguities may be mitigated by careful experimental design, but the neurophysiological interpretation of correlation patterns is an unsettled issue.

Besides the scientific value of studying the neural activity associated with preparation to respond and the subsequent left or right-handed response to numeric information, the bimanual experiment described in this Report is designed to provide a data base for refining the NCP Analysis and investigating some aspects of the neurophysiological interpretation of correlation patterns. In addition to inter-channel, zero-lag correlation, NCP Analysis can employ other measures such as multi-lagged correlation and covariance, and single channel power, all in specific frequency bands. Preliminary studies described in last year's Final Report have revealed significant information with such measures. A major goal during the coming year is to explore and resolve some of these issues.

II. Piloting and Recording of a Bimanual Perceptuomotor Study

A. Overview.

We are applying a new method, called Neurocognitive Pattern (NCP) Analysis, to measure spatial neurocognitive electrical processes of the human brain during goal directed activities. NCP Analysis has been successfully applied in four studies, and results so far are quite promising. An area of particular interest is neurocognitive changes associated with learning. In considering possible experimental designs, it became evident that the concept of 'learning' is fuzzy and encompasses numerous phenomena. Animal models were found to be misleading in major ways because of the computational and adaptive superiority of human brains. For example, several years ago we piloted a study which attempted to examine learning in the form of adaptation to changing response criteria in a simple visuomotor task. We found that people were able to adapt too quickly to the changes to provide a sufficient data-base. In a sense, the participants quickly 'automated' the process of adapting to changes. A more difficult perceptuomotor learning paradigm was designed and implemented, but it suffered from excessive complexity. Thus even if they were measured, putative neurocognitive patterns of 'learning' could not be definitively identified with perceptual, cognitive or motor aspects of the task. This would have rendered such results of little fundamental interest. Further consideration led us to conclude that direct assaults on this difficult problem must be postponed until a number of prerequisite issues were addressed. Before subtle aspects of perceptuomotor and cognitive learning could be meaningfully examined, it was necessary to: 1) further refine and validate our new method of NCP Analysis on data from simpler experiments; 2) develop effective digital filters for eye movement (and muscle potential) contamination of brain potentials; 3) improve the spatial resolution to resolve patterns over inferior and superior parietal and dorsolateral prefrontal cortices (this would require at least 49 recording electrodes); and 4) measure the neurocognitive patterns associated with preparation, attention and 'updating' which are constituent processes of learning. Accordingly, it seemed prudent to conduct a preliminary study of a very basic issue: a comparison of the patterns of mass neuroelectric activity associated with the expectation, performance and 'updating' of a right and left-handed visuomotor task.

We have designed and implemented a study intended to delineate the time-varying foci of neuroelectric activity associated with:

1) <u>preparation</u> to respond with either the left or right hand using a hand-cued paradigm;

2) <u>performance</u>, with right and left hands, of a brief, difficult numeric visuomotor task; and

3) <u>'updating'</u> when presented with feedback about the accuracy of a response.

This experiment will also provide a high-quality data-base for further refinement of NCP Analysis. Studying these three issues will require analyzing brain potentials to cue, stimulus, response and feedback. This will represent an expansion of the temporal extent of our analysis from about one second to six seconds.

B. Task Development.

By June 1, 1983, six full pilot recordings and 17 preliminary screenings were conducted using a cued bimanual numeric judgment paradigm. The basic task was the numeric visuomotor judgment task first reported in Science, 21 August, 1981 (213:918-922). It involves the execution of a precise contraction of the index finger in response to visually presented single digit number stimuli on a linear scale of pressures from 1 to 9. The design and instrumentation allow a high degree of control over stimulus, response, and performance-related factors. The stimulus is preceded by a cue symbol (V) which indicates the responding hand by the direction of its tilt, either to the right or left. The stimulus number itself is also tilted in the direction of the hand which is to make the response, and the participants are instructed to attend the cue so that appropriate responses could be made quickly and accurately as soon as the stimulus number appeared (see below).

Feedback indicating the exact pressure exerted is presented one second after response completion. If the response is sufficiently accurate, the feedback number is underlined, indicating a "win". The error tolerance (ie. degree of accuracy required for a win) is adaptive; it is computed as a continuous moving average of the actual error on the preceeding five trials. This technique equalizes task difficulty across the session, and also serves as an index of a person's current skill level. After completion of each block of 17 trials, a display is presented showing the final size of the error tolerance and the amount of bonus money won on that block (about 5 cents for each win).

The electrode montage consisted of 21 EEG channels (Fz, aF1, aF2, F7, F8, aCz, Cz, C3, C4, C5, C6, Pz, P3, P4, aP5, aP6, T5, T6, Oz, aO1 and aO2) referenced to linked mastoids and recorded with tin alloy electrodes affixed to a specially fabricated nylon mesh cap (Electrocap Int.). Horizontal and vertical EOG were recorded with Ag-AgCl electrodes, as was the EMG activity of the flexor digitorum muscle of both right and left hands. All signals were lowpass filtered at 100 Hz and digitized at 256 Hz by the PDP-15 computer which ran the experiment.

1. Design #1 (P#1).

In order to study the neuroelectric patterns associated with preparation to execute either a right or a left-handed response, the design must allow an inference of the existance of a hand-specific preparatory set in the interval between the cue and stimulus. This was done with a miscuing technique wherein a randomly ordered 20% of the cues are invalid. That is, the responding hand indicated by the

stimulus is opposite to the hand indicated by the cue. A person is instructed to always respond with the hand indicated by the tilt of the stimulus number. The existance of a hand-specific preparatory set is then inferred by the 'costs' (lengthing of reaction time (RT) and increase in error rate) in the miscued trials. This method has been used to infer the existance of modality-specific, position-specific and task-specific preparatory sets in various paradigms (Posner, 1978), and in our laboratory in an auditory-visual bimodal attention version of the numeric task used here.

One person was recorded in this 'move-to-miscues' version of the bimanual task (total 403 trials; cue-to-stimulus interval = 1.5 sec), and substantial 'costs' due to miscueing were observed (Table 1). Considered together, the increase in average response time in miscued right and left handed trials was 68 msec, a 12.3% lengthening of the average RT of the correctly cued trials. The error rate (proportion of 'lose' trials) increased from 56% in correctly cued trials to 68% in miscued trials.

Average stimulus-registered event-related potentials (ERPs) showed a 30% increase in amplitude of the P3 peak in the miscued trials. P3 peak latency was about 375 msec in all correctly and incorrectly cued conditions. This P3 enhancement to the violation of the cue-indicated expectancy as to responding hand was a further confirmation of the existance of a hand-specific preparatory set in the pre-stimulus interval. However, Design #1 was deemed unsatisfactory because attention to the cue could not be confirmed on <u>each</u> trial.

2. <u>Design #2</u> - <u>Move/no-move (P's #2-5).</u>

The task and recording methods were the same, except that a person was required to make <u>no response</u> on miscued trials. (EMG channels on each no-move trial were inspected to assure that no flexion or extention movements were made.) This design will allow a 'within hand' NCP Analysis of move and no-move trials to delineate the foci of post-stimulus processing for each hand seperately. This approach was successfully used in our recent study of a visuospatial task (<u>Science</u>, 1983, 220:97-99 -- see Sections III and IV), and is likely to aid in interpreting the direct NCP Analysis of right versus left-handed move trials. This latter point is particularly important, since we do not expect the neurocognitive patterns of left-handed responses to be merely mirror images of those associated with right-handed movements (see discussion of movement-related ERPs below).

Four practiced, right-handed adults performed from 355 to 1000 trials of this design (total 2151 trials). The cue-to-stimulus interval for P's #2-4 was 1.5 sec, and for P#5 it was 1 sec. Behavioral data for the move (correctly cued) conditions is given in Table 2 (which includes the correctly cued trials of P#1). Average response times, error rate, and error tolerance (as an indication of skill level) were similar for both left and right-handed trials. Also, the standard deviations of response times were similar within and across persons. Thus performance-related factors were equivalent across hands.

C. ERP Description.

1. Stimulus Related Peaks.

In NCP Analysis, average ERPs are computed for each person seperately in order to determine the onset and offset times of the post-stimulus analysis intervals. One such interval will be centered on the N1-P2 peak complex, another on the average P3 peak latency, and a third on the movement-related potential shift, registered retrograde to the movement onset in each trial.

The stimulus-registered averages of P#4 are shown in Figures 1-4. In all persons recorded, the N1 peak was largest at the lateral temporal sites (T5 and T6), smaller at the lateral occipitals (aO1 and aO2), and for P's #3, 4 and 6 barely visible at the midline occipital placement (Oz). This may have been due to the small visual angle (<1 degree) subtended by the stimuli, in which case the presumed cortical generators for foveated stimuli would be buried in the calcarine fissure and project tangentially to lateral sites. For P#5 the stimuli were doubled in size and their line thickness increased, resulting in a more robust midline peak. The P2 peak is overlapped by the sharp resolution of the fronto-centrally dominant cue-to-stimulus CNV, and was not clearly visible in most people (see next section).

The P3 peak was visible in all move and no-move conditions with peak latencies from 320 to 550 msec. Amplitudes were larger in the no-move (miscued) conditions for all persons, and the duration of positivity was longer. Several distinct peaks were visible as late as 750 msec.

2. Movement Related Potentials.

In move trials the positive peak complex was followed by a negative-going slow potential shift (Figs. 1-4). Midline distribution was maximal at fronto-central sites (usually aCz), and of nearly equal amplitude in right and left hand conditions. Its lateral topography, however, varied between hands. For right-handed responses, it exhibited a strong left-sided lateralization, usually maximal at C3. For left-handed responses, the lateralization did not reverse; rather, it exhibited either a smaller left-sided lateralization than right-handed trials, or else no distinct lateralization. The response-registered averages (Figs 5 and 6) show a similar pattern. (The only exception to this was in P#2). The overall picture suggests that left-handed movement-related activity is not merely a mirror image of right-handed activity, in spite of the equivalence of response and performance-related factors between hands. For this reason the 'within hand' NCP comparison of move versus no-move trials will be a prerequisite step in analysis. The focal patterns of neural activity determined for each hand seperately will aid in interpreting the results of the direct NCP comparison of left versus right hand conditions.

3. Cue-Related Waveform.

The existance of a cue-to-stimulus contingent negative variation (CNV) was evident in the fronto-centrally dominant displacement of the pre-stimulus baseline in all recordings. CNV activity is to be expected in a cued paradigm such as this, and may well be an integral part of the process of task preparation. To examine the effects of the cue-to-stimulus interval on the CNV, and the effects of its resolution on the post stimulus ERP waveform, one person was recorded (P#6) in the right hand condition at two intervals. In the first run the interval was 2.5 sec and in the second run it was 1 second. The sharp positive-going CNV resolution, extending from 125 to 165 msec post-stimulus for both intervals, was larger in magnitude for the longer (2.5 sec) interval. At anterior sites it partially overlaped the P234 peak. Response times and error rates were equivalent for the two intervals. The error tolerance for the shorter interval trials showed an improvement in performance (which may have been due to a learning effect). It was concluded that lengthening the cue-to-stimulus interval will not reduce the effects of the CNV and its resolution, and we are therefore employing the shorter (1 sec) interval in the formal recordings.

D. Final Design.

The task is the cued bimanual move/no-move task, with a 1 sec cue-to-stimulus interval. Visual stimuli have been enlarged to just under 2 degrees visual angle and drawn with thicker lines. The electrode montage has been enlarged to 26 channels (Fz, F3, F4, aF1, aF2, aCz, aC3, aC4, Cz, C3, C4, C5, C6, aP1, aP2, aP5, aP6, Pz, P3, P4, T5, T6, Oz, aO1, aO2 and aOz) referenced to aPz. A common average reference will be computed off-line. Signals are lowpass filtered at 50 Hz and digitized at 128 Hz. Digitization begins .75 sec before the cue and extends to 1 sec after onset of feedback. Editing for artifact will include the feedback epoch to allow an analysis of neural patterns such as those accompanying feedback to accurate and inaccurate trials. The main analyses will be: 1) move vs. no-move trials for right and left hands seperately, 2) right hand vs. left hand move trials, and 3) the cue-to-stimulus interval for left-vs right hand cues.

E. Participant Screening Program.

Twenty-three candidate participants have been screened to date. The screening procedure consists of 200 practice trials and 200 test trials of the bimanual task. The test trials are recorded from Fz, Cz, Pz, aO1 and aO2 (to observe the post-stimulus ERP waveform), T1 and T2 (to assess amount of EMG from temporalis muscles), and diagonally placed EOG electrodes. Eleven candidates who were unable to perform satisfactorally were excused from further participation.

F. Formal Recordings.

Six formal test recordings have been completed to date, using the 26 channel EEG montage described above. About 900 trials were recorded from each person. Trials with response times longer than 1.25 sec,

poor response movements, and no-move trials on which a response is made are automatically rejected. Data attrition due to these sources, and to instrumental and eye-movement artifacts, is about 25%. Thus we have obtained about 3600 useable trials. The remaining data-base should be completed with the recording of 5 more persons.

Table 1 "Costs" in response time and error rate due to miscueing (miscues random 20%; 10% right hand, 10% left hand) (P#4 - MOSPI)

		Correctly cued				Miscued				Costs of miscueing			
		Right Hand		Left Hand		Right Hand		Left Hand		Right Hand		Left Hand	
Run #	Number of Trials	$\overline{R.T.}$ msec (S.D.)	Lose %	$\overline{R.T.}$ msec (S.D.)	Lose %	$\overline{R.T.}$ (S.D.)	Lose %	$\overline{R.T.}$ (S.D.)	Lose %	increase in $\overline{R.T.}$ (msec)	increase in Lose %	increase in $\overline{R.T.}$ (msec)	increase in Lose %
1	205	547 (165)	48	487 (194)	53	617 (161)	65	563 (258)	71	70	17	76	18
2	198	617 (190)	54	559 (147)	47	695 (157)	60	607 (149)	53	78	6	48	6
$\overline{X}$	Total Trials 403	582 (177)	51	523 (170)	50	651 (159)	62.5	585 (203)	62	+74 msec	11.5%	+62 msec	+12%

Table 2 Reaction times, error rate (Lose %), and average error tolerance (as a performance index on a scale of 1:100 units) for correctly cued (move) tirals (P's #1-5)

			Right hand			Left hand		
P#	Run #	Number of Trials	$\overline{RT}$ (S.D.) msec	Lose %	Error Tolerance	$\overline{RT}$ (S.D.)	Lose %	Error Tolerance
#1	1	205	547 (165)	48	9.0	487 (194)	53	15.1
	2	198	617 (190)	54	6.2	559 (147)	47	11.8
#2	1	198	770 (167)	54	7.8	778 (165)	55	10.3
	2	171	795 (182)	57	10.4	810 (232)	60	15.6
#3	1	205	783 (167)	55	11.7	852 (222)	51	12.2
	2	150	773 (144)	52	6.4	786 (130)	51	10.3
#4	1	205	609 (122)	60	13.8	586 (126)	60	7.6
	2	205	673 (80)	54	10.7	683 (107)	50	7.0
#5	1	205	625 (95)	50	13.8	660 (124)	52	7.8
	2	205	625 (142)	54	8.7	625 (97)	49	9.8
	3	197	650 (146)	48	8.1	640 (129)	53	10.9
	4	205	669 (136)	49	12.4	636 (159)	61	10.5
	5	205	660 (169)	49	9.8	605 (170)	52	9.5
$\overline{X}$ (average $\overline{S.D.}$ across P's)		Total Trials 2554	676 msec (146)	52.6%	9.9	655 msec (154)	53.3%	10.6

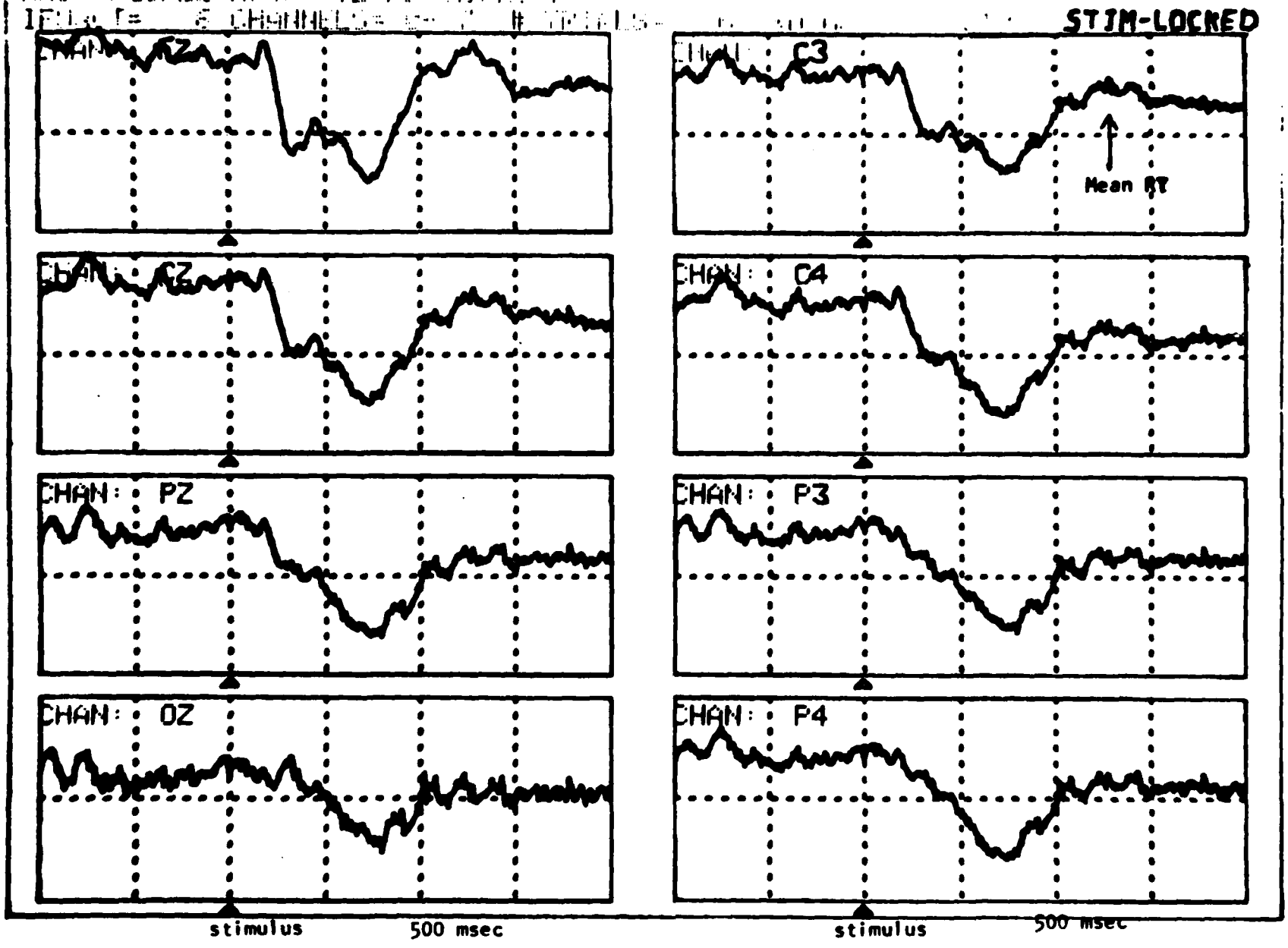

Figure 1a - Right hand move condition. Average ERPs from P#4 (8€ trials, .1 to 100 Hz passband.)

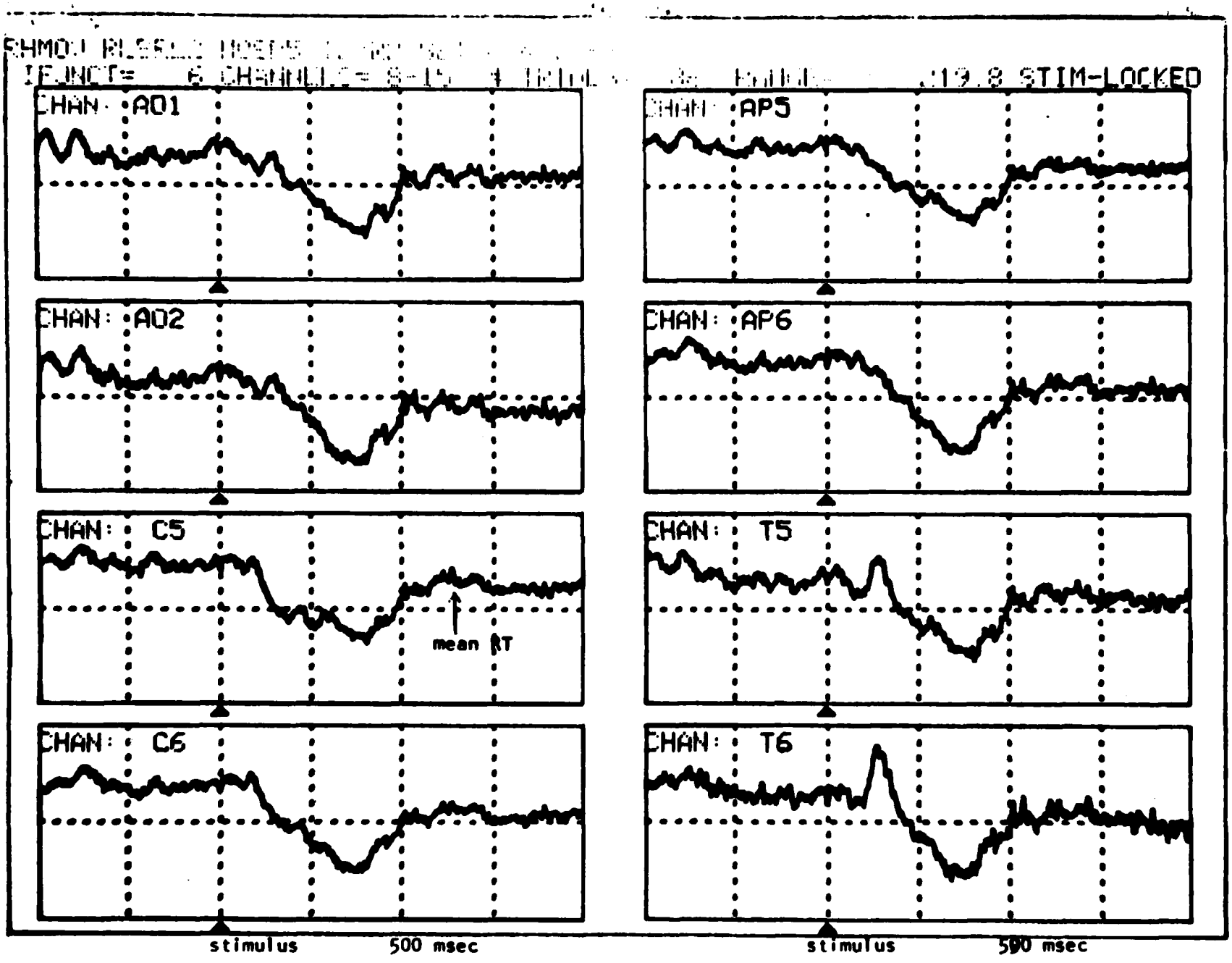
STIM-LOCKED
CHAN: AO1
CHAN: AP5
CHAN: AO2
CHAN: AP6
CHAN: C5
CHAN: T5
mean RT
CHAN: C6
CHAN: T6
stimulus
500 msec
stimulus
500 msec

Figure 1b

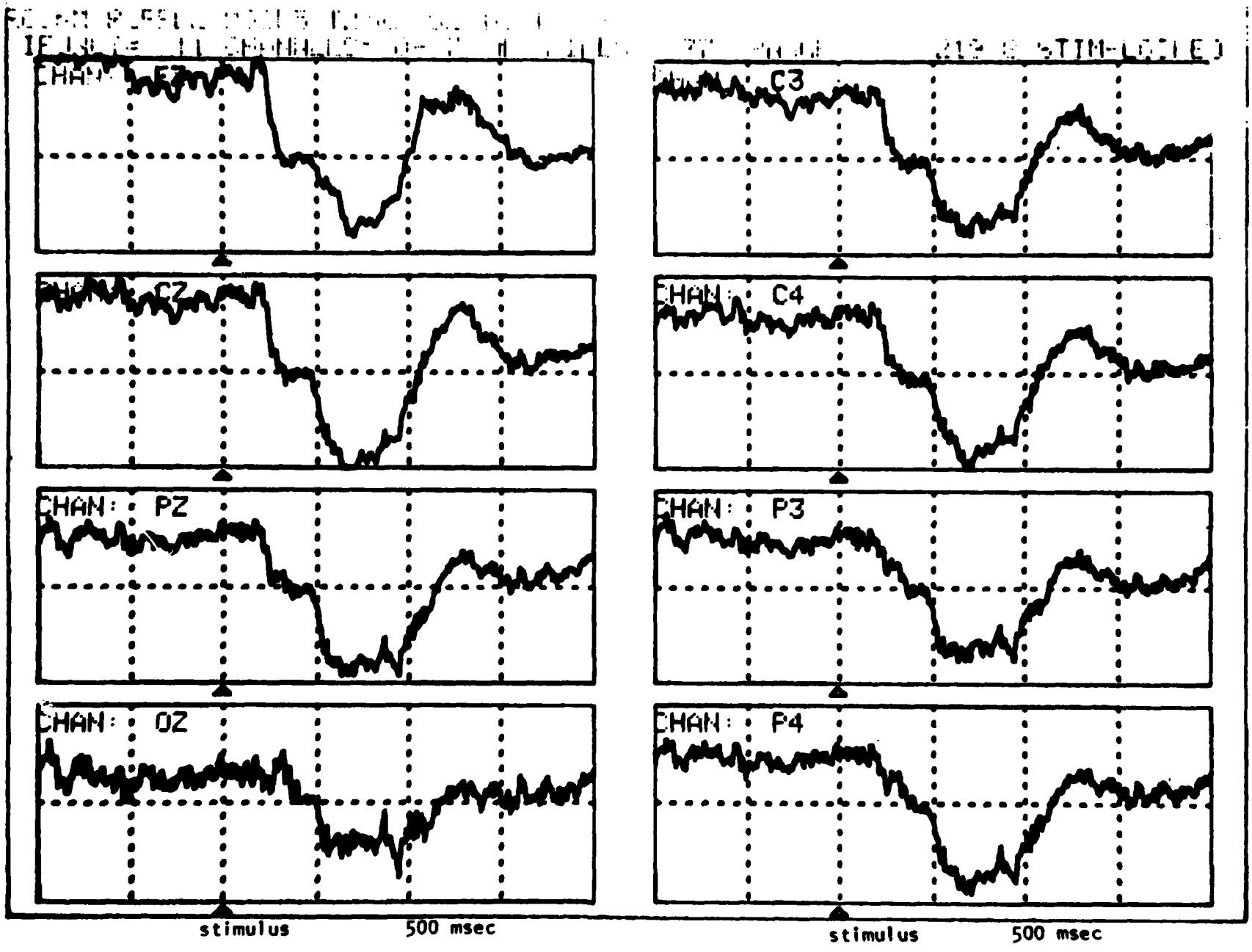

Figure 2a - Right hand cued no-move condition. (37 trials)

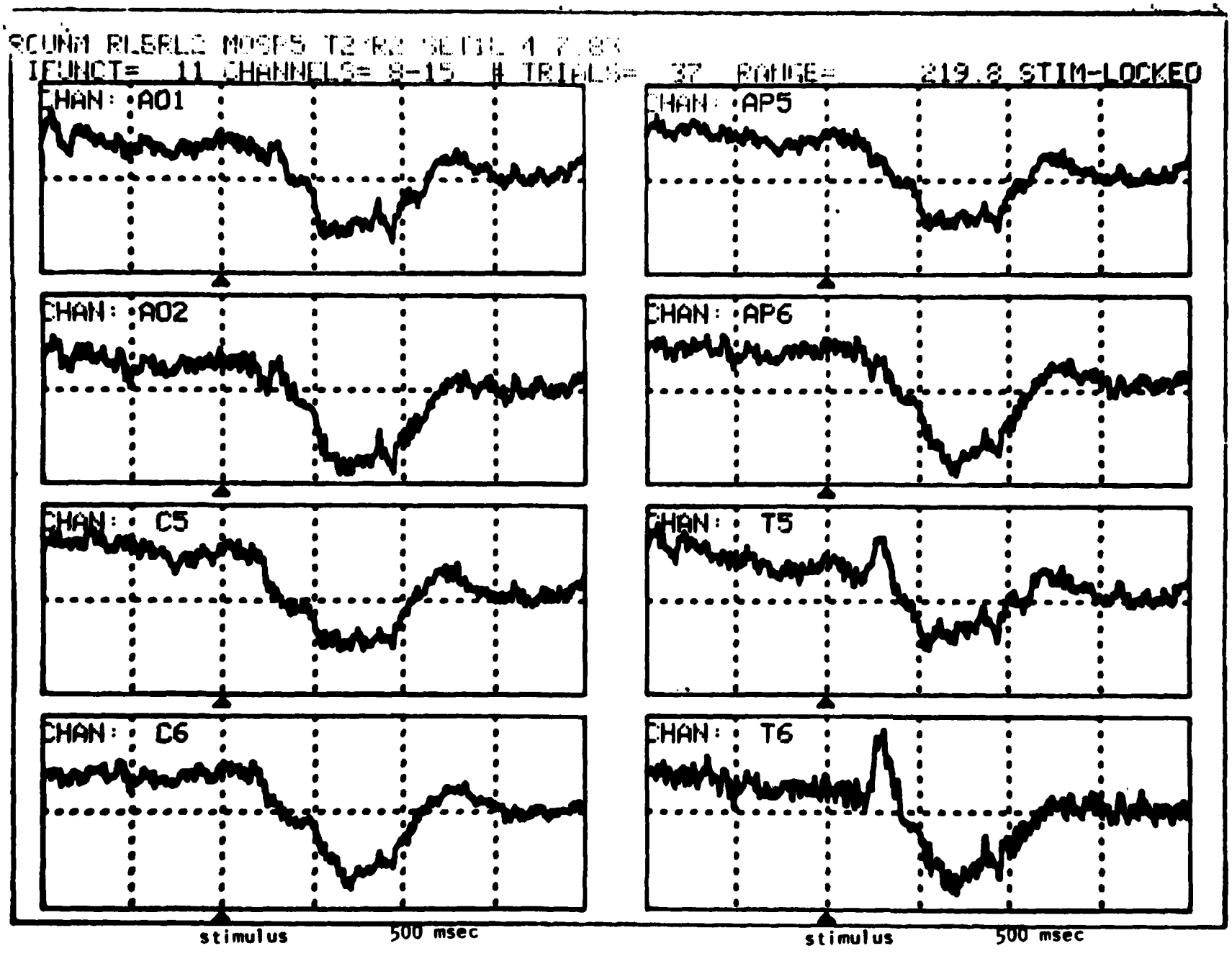
FUNCT= 11 CHANNELS= 8-15 # TRIALS= 37 RANGE= 219.8 STIM-LOCKED
CHAN: A01
CHAN: A02
CHAN: C5
CHAN: C6
CHAN: AP5
CHAN: AP6
CHAN: T5
CHAN: T6
stimulus
500 msec
stimulus
500 msec

Figure 2b

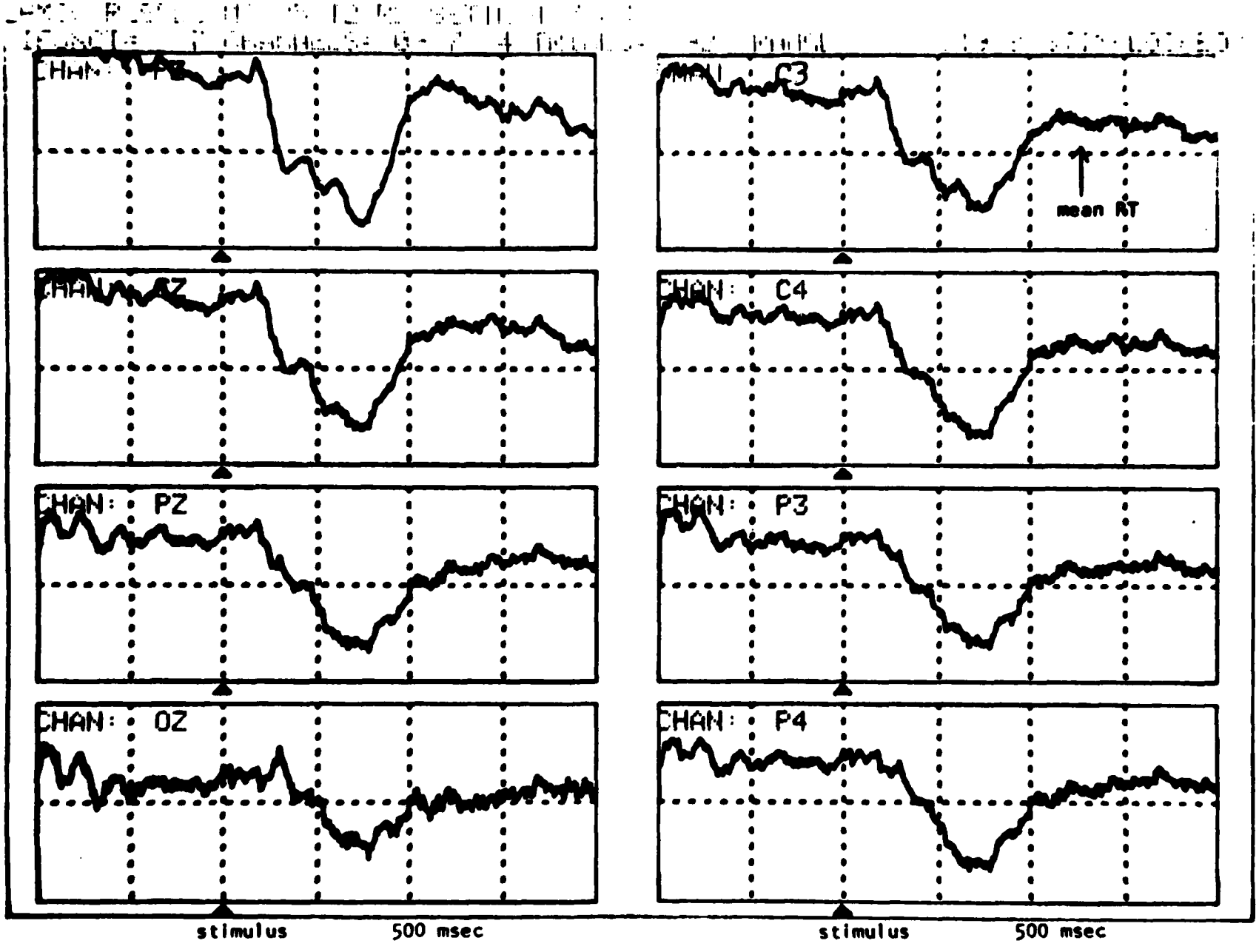

Figure 3a - Left hand move condition (92 trials from P #4).

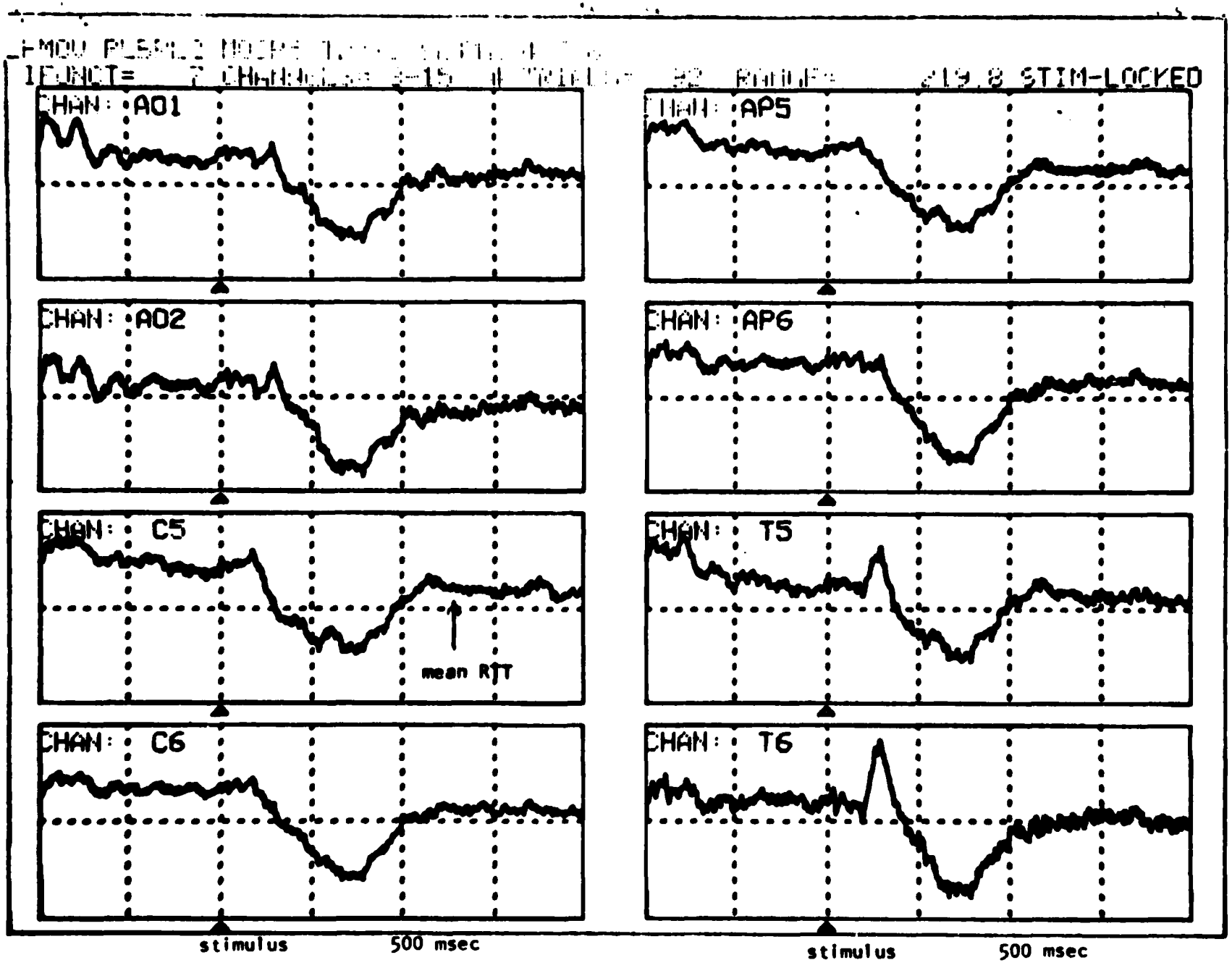
CHAN: A01
CHAN: A02
CHAN: C5
mean RTT
CHAN: C6
stimulus
500 msec
CHAN: AP5
CHAN: AP6
CHAN: T5
CHAN: T6
stimulus
500 msec

Figure 3b

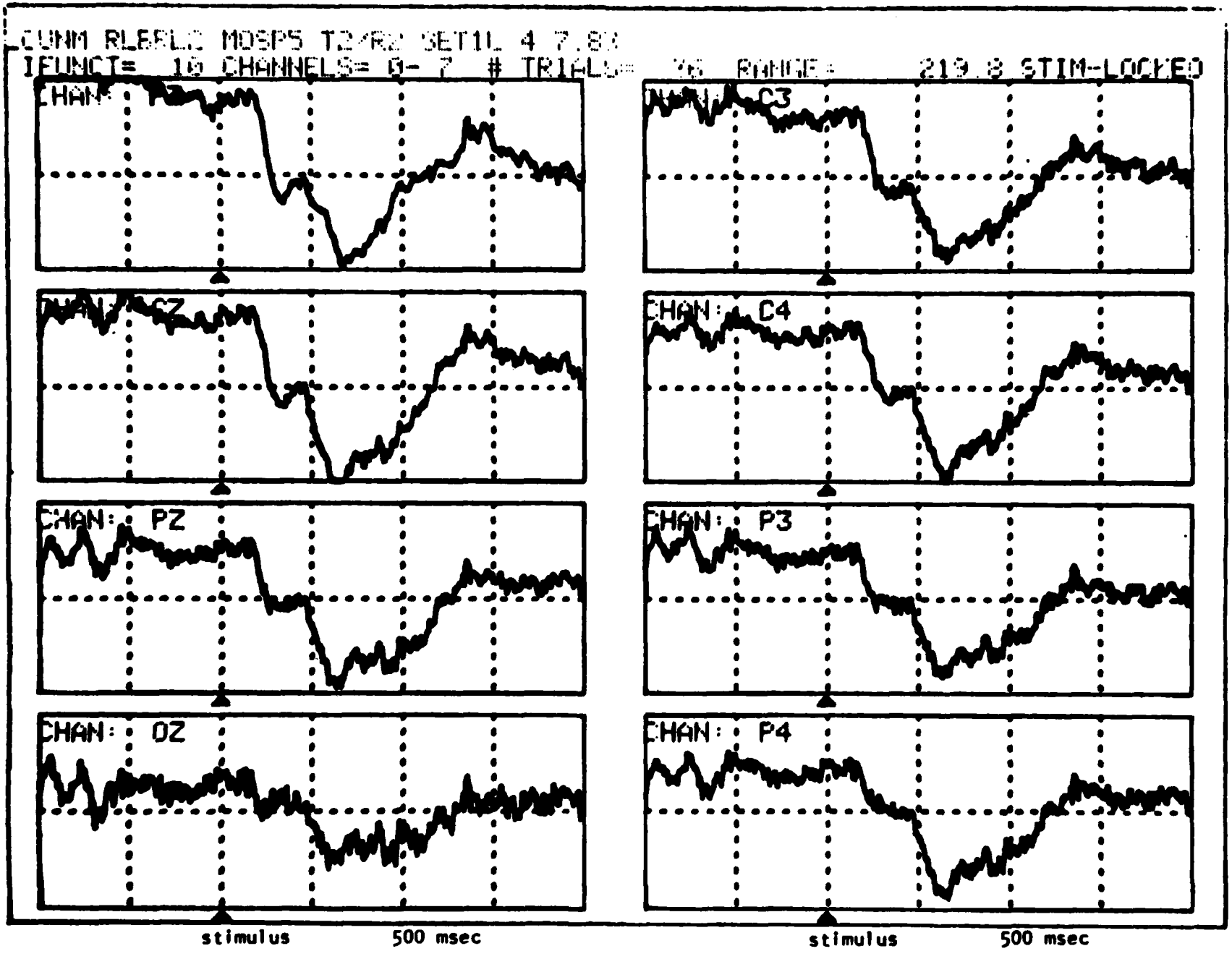

Figure 4a- Left hand cued no-move condition (36 trials).

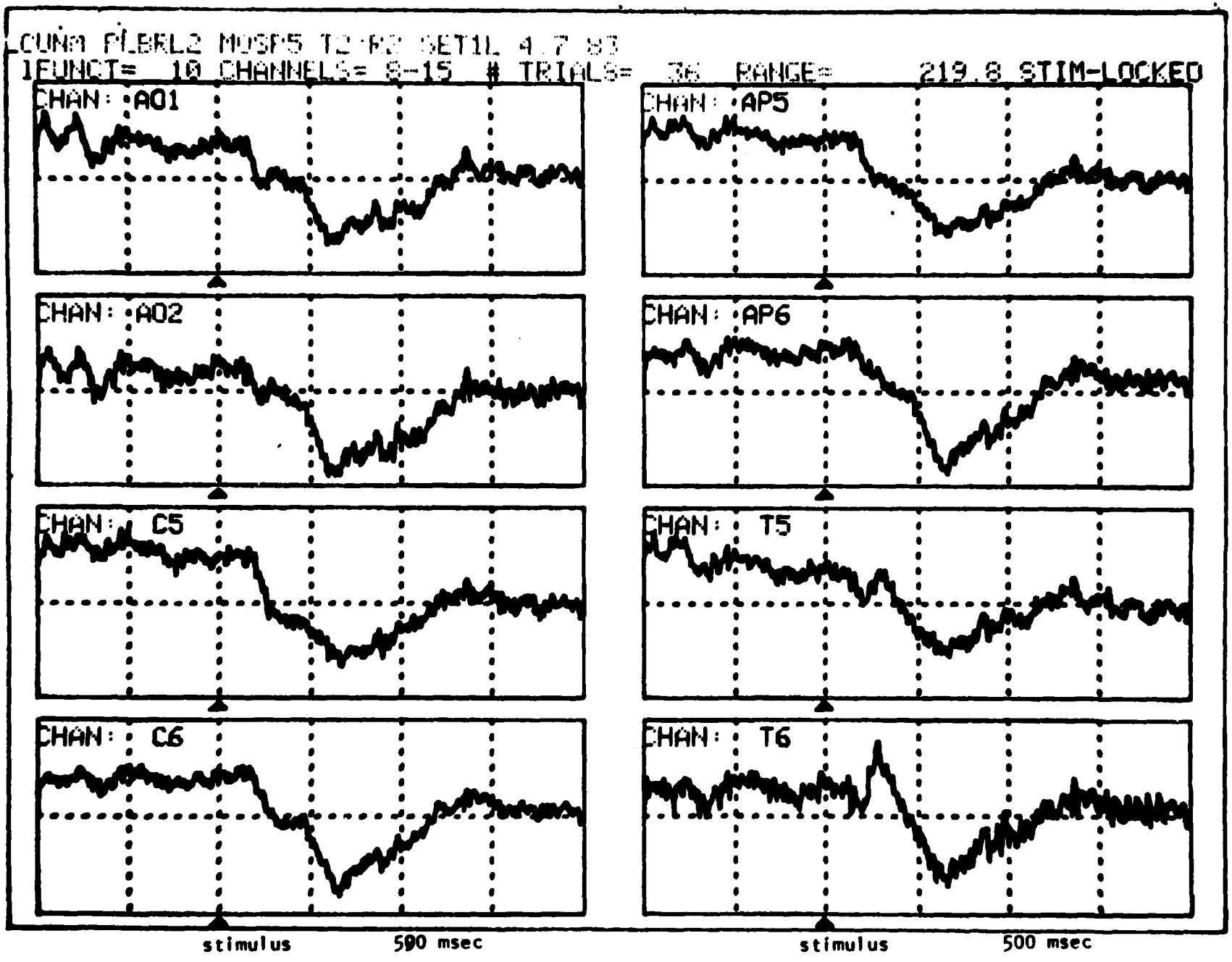
CHAN: A01
CHAN: A02
CHAN: C5
CHAN: C6
CHAN: AP5
CHAN: AP6
CHAN: T5
CHAN: T6
stimulus
500 msec
stimulus
500 msec

Figure 4b

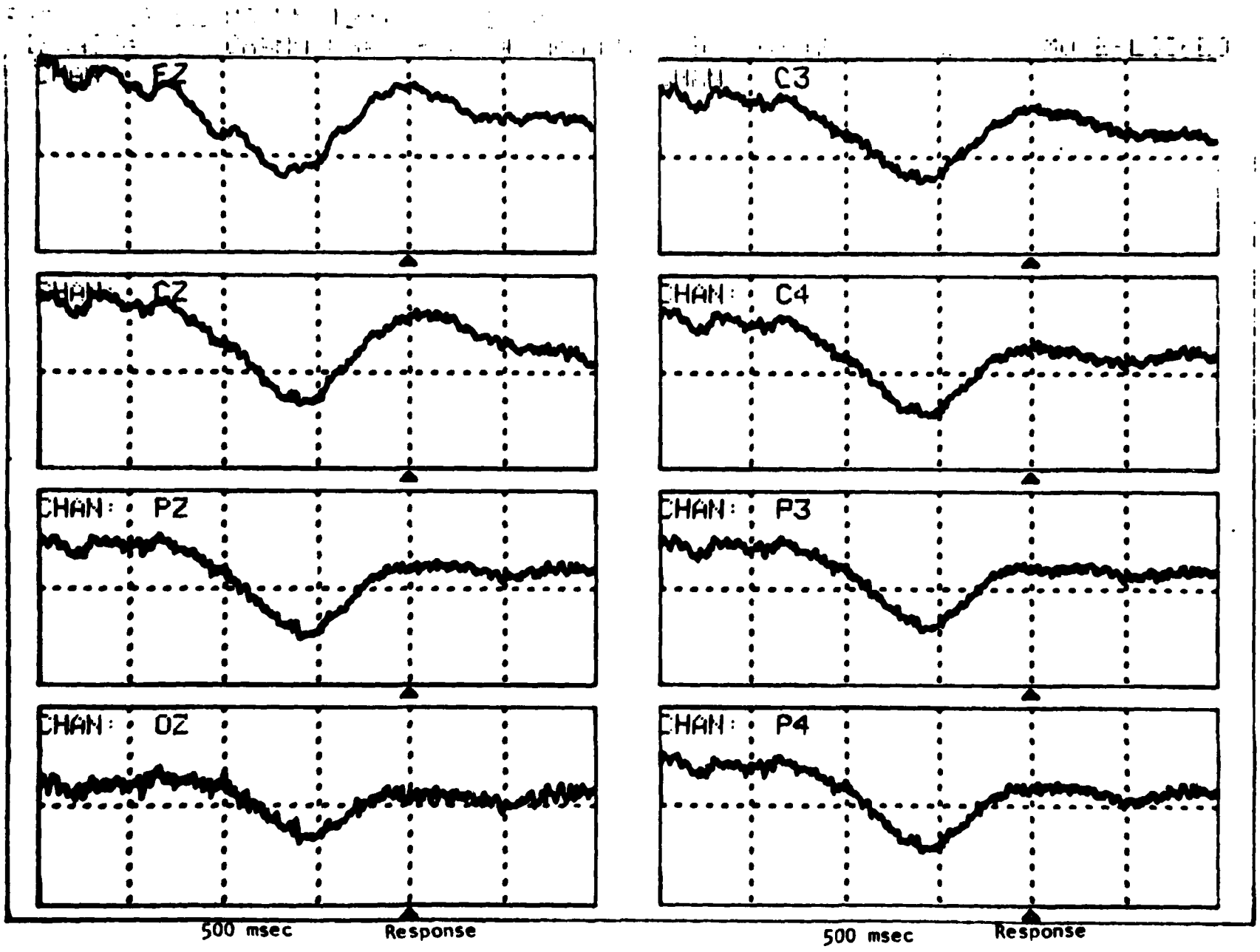

Figure 5a - Right hand movement-registered ERPs from P #4 (86 trials).

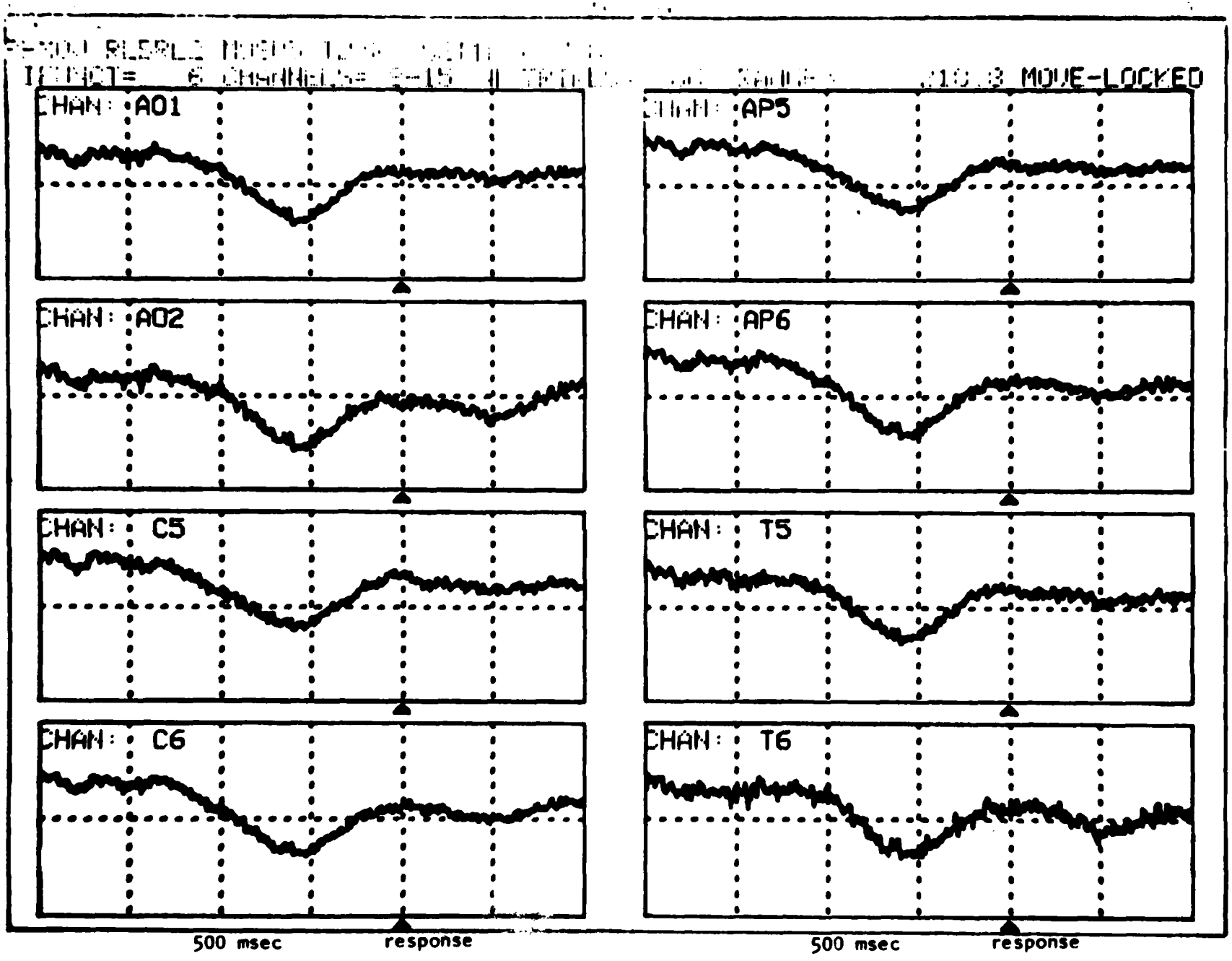
MOVE-LOCKED
CHAN: A01
CHAN: A02
CHAN: C5
CHAN: C6
CHAN: AP5
CHAN: AP6
CHAN: T5
CHAN: T6
500 msec
response
500 msec
response

Figure 5b

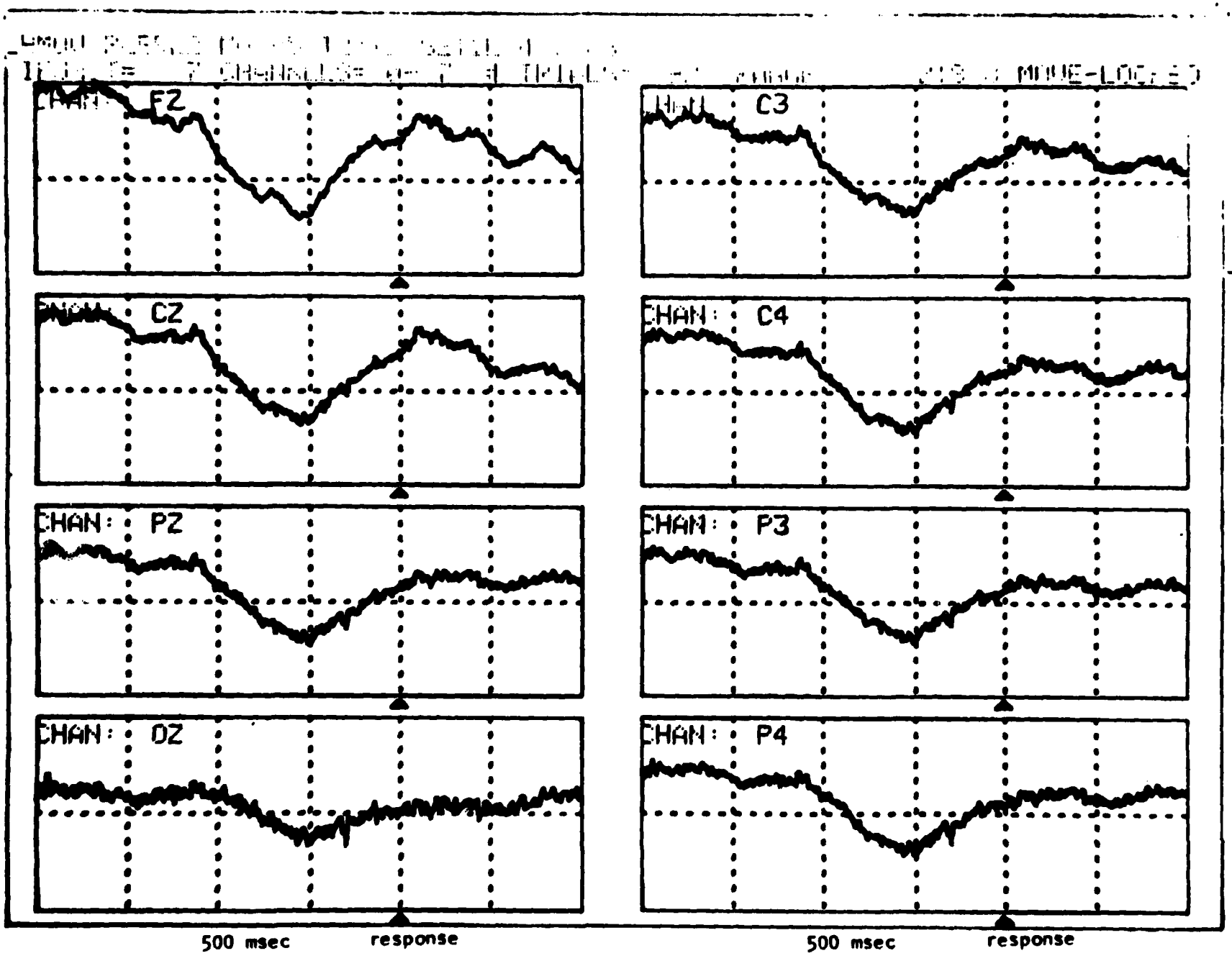

Figure 6a - Left hand movement registered ERPs from P #4 (92 trials).

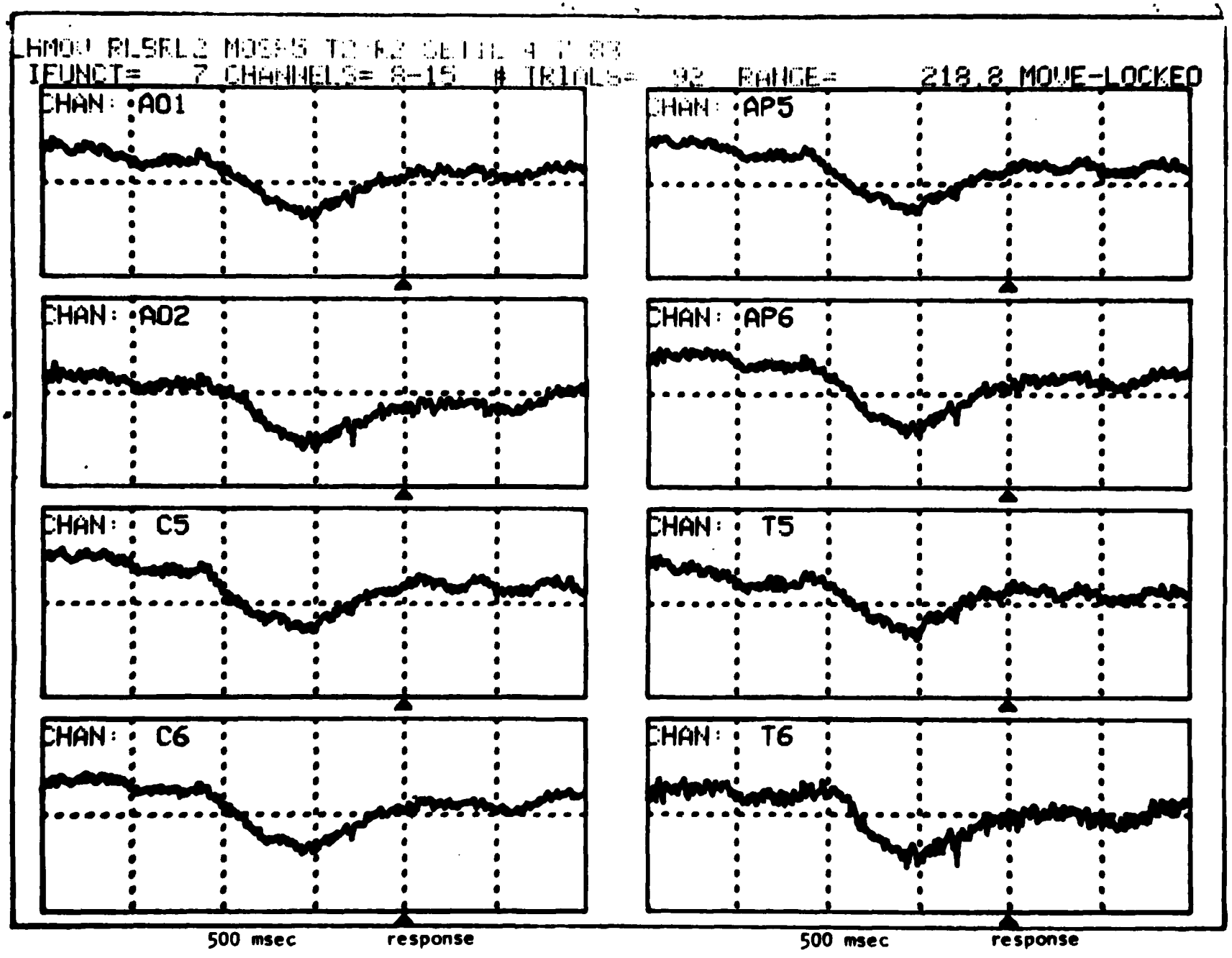
IFUNCT= 7 CHANNELS= 8-15 # TRIALS= 92 RANGE= 218.8 MOVE-LOCKED
CHAN: A01
CHAN: AP5
CHAN: A02
CHAN: AP6
CHAN: C5
CHAN: T5
CHAN: C6
CHAN: T6
500 msec
response
500 msec
response

Figure 6b

Reprint Series
1 April 1983, Volume 220, pp. 97–99

SCIENCE

Shadows of Thought: Shifting Lateralization of Human Brain Electrical Patterns During Brief Visuomotor Task

Alan S. Gevins, Robert E. Schaffer, Joseph C. Doyle, Brian A. Cutillo, Robert S. Tannehill, and Steven L. Bressler

Shadows of Thought: Shifting Lateralization of Human Brain Electrical Patterns During Brief Visuomotor Task

Abstract. *Dynamic spatial patterns of correlation of electrical potentials recorded from the human brain were shown in diagrams generated by mathematical pattern recognition. The patterns for "move" and "no-move" variants of a brief visuospatial task were compared. In the interval spanning the P300 peak of the evoked potential, higher correlations of the right parietal electrode with occipital and central electrodes distinguished the no-move task from the move task. In the next interval, spanning the readiness potential in the move task, higher correlations of the left central electrode with occipital and frontal electrodes characterized the move task. These results conform to neuropsychological expectations of localized processing and their temporal sequence. The rapid change in the side and site of localized processes may account for conflicting reports of lateralization in studies which lacked adequate spatial and temporal resolution.*

Many investigators have reported that brain activity is lateralized during cognitive tasks. Advanced radiological methods reveal relative localization and lateralization, but cannot resolve temporal sequencing because of the long time required for observation. Studies of ongoing, background electrical activity do not reveal split-second changes in neurocognitive patterns, and those that have reported lateralization of neurocognitive activity have been questioned on methodological grounds (*1–6*). Although the components of averaged event-related potentials (ERP's) may indicate the sequencing of some neurocognitive processes, they have not revealed consistent, robust signs of lateralization, even for language (*7*). Conclusions derived from patients with focal brain lesions or with "split-brains," cannot be directly extended to normal subjects. Lateralized processes inferred from reaction time differences to hemifield or dichotic stimulation have also been questioned on methodological grounds (*8*). These factors have undoubtedly contributed to conflicting reports of lateralization of brain activity.

To observe the spatial patterns and sequencing of neurocognitive activity, we have developed a new method called neurocognitive pattern (NCP) analysis. In NCP analysis the average ERP's of each person are used to determine the time intervals of task-related neural processes. Within these intervals the similarity of brain-potential waveshapes over the scalp is measured on a single-trial basis by computing the cross-correlation coefficient between paired combinations of electrodes. Although the neuroanatomic origin and neurophysiological significance of these correlations is not known, it has been suggested that cognitive activity may be associated with characteristic scalp correlation patterns (*9*). However, task-related electrical signals from the brain are spatially smeared in transmission to the scalp and are embedded in background activity. Since linear statistical methods were not effective in dealing with these obstacles, we used a more powerful analysis called trainable classification-network mathematical pattern recognition (*2, 3, 10–13*). For this method, artificial intelligence algorithms are used to extract patterns of correlation that differ between two conditions with no assumptions about the distribution of correlation values. The algorithm is first applied to a labeled subset of the experimental data called the training set, and the invariant patterns (classification functions) found are then verified on a separate unlabeled subset of data called the test set. If the classification functions can significantly separate the test set into the two conditions, the extracted patterns have intrinsic validity.

Previously we reported the existence of complex, rapidly changing patterns of brain-potential correlation involving many areas of both hemispheres that distinguished numeric and spatial judgments in a visuomotor task (*13*). Since the sequencing of neurocognitive differences between numeric and spatial processing is not definitely known, the complex patterns were difficult to interpret. The present experiment was designed to clarify this situation by highlighting presumably localized neural processes. In comparing two types of spatial judgment, the common activity of brain areas should cancel, revealing differences in the right parietal area presumed to mediate spatial judgments. The right-handed finger response in one task was designed to elicit lateralized activity of the left central motor area.

In this study a person estimated the distance a "target" should be moved to intersect a displayed arrow's trajectory. The "move" task required pressure of the right index finger on a transducer with a force proportional to that distance (*14*). In the "no-move" task the arrow pointed directly at the target, and no pressing was required (pseudorandom 20 percent of trials). Thus, the spatial judgment and response differed between tasks, while gross stimulus characteristics were the same.

Nine right-handed, healthy adults (eight males, one female) participated in the study. The average response initiation (muscle potential onset) time for the move trials was 0.59 second (standard deviation, 0.19; mean of standard deviations within persons, 0.24). Brain potentials were recorded from 15 scalp electrodes and referenced to linked mastoids (Fig. 1A) (*15*). Vertical and horizontal eye movements, muscle potentials from the responding finger, and the output of the force transducer were also recorded. The data were edited to remove trials with artifacts, and a set of 1612 correct, representative trials (839 move, 773 no-move) was formed. Averaged ERP's were computed for all electrodes (Fig. 1B), and *t*-tests and analyses of variance (ANOVA's) were performed (*16, 17*).

Cross-correlations were computed between 91 paired combinations of the 15 electrodes for each trial in each of three 175-msec intervals (Fig. 1B). Two intervals spanned the N100–P200 and P300 ERP peaks, and the third (RP) interval spanned most of the readiness potential (in the move task). The centerpoint of each interval was determined for each person (*18*). The correlations were standardized within persons, within electrode pairs (mean, 0; standard deviation, 1), and then grouped across people. The *t*-tests and ANOVA's of single-trial correlations did not distinguish meaningful differences in between-task spatiotemporal patterns.

Mathematical pattern classification was then applied to the single-trial correlations of all nine people to search for subtle between-task differences in each interval. To make the results anatomically interpretable, we performed the search separately on each of 15 sets of electrode pairs. Each set consisted of the correlations of a particular electrode with ten other electrodes (Fig. 1C). For each interval, the electrode set that distinguished conditions on the test set with the highest significance level (*19*), and the most prominent correlations for that electrode set (*20*), were diagramed.

In the N100–P200 interval, correlations of the midline parietal electrode distinguished the tasks ($P < .001$) (Fig. 2A). In the P300 interval, correlations of the right parietal electrode with the midline occipital and precentral electrodes were greater in the no-move task, while correlations of the right parietal with the right central electrode were greater in the move task ($P < 5 \times 10^{-5}$) (Fig. 2B). In the RP interval, correlations of the left central electrode with the midline frontal and occipital electrodes were greater in the move task, while correlations of the left central electrode with the midline parietal electrode were greater in the no-move task ($P < 5 \times 10^{-6}$) (Fig. 2C).

The right parietal locus of between-task difference in the P300 interval may reflect a lateralization of activity distinguishing the two types of spatial judgment (*21*) or the difference between movement estimation in the move task and the cancellation of response in the no-move task. The left central focus of difference in the RP interval 135 msec later may reflect the preparation and initiation of the movement of the right index finger. In contrast, the pattern of difference in the N100–P200 interval was not lateralized.

These results may help explain conflicting reports of brain-potential lateralization. In many studies, various "verbal-analytic" and "spatial" tasks 1 minute or more in duration have been associated with relative left and right hemisphere EEG activity (*1–6*). However, it

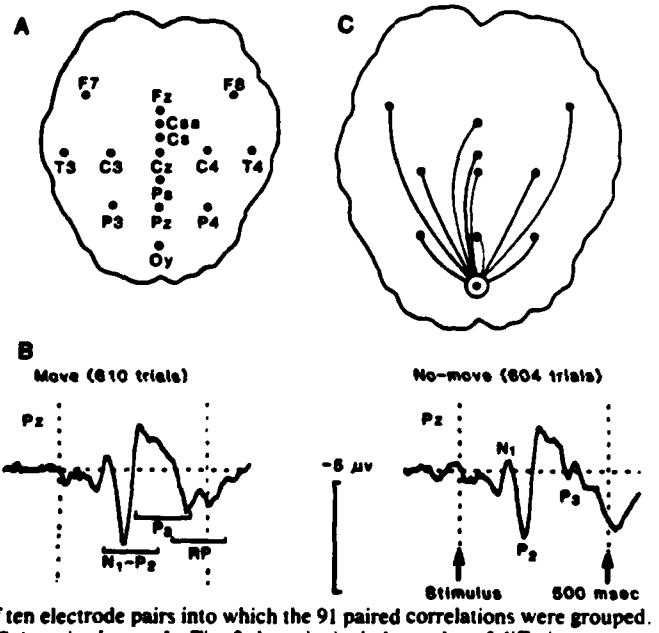

Fig. 1. (A) Montage of 15 electrodes. Nonstandard placements are intended to overlie cortical areas of particular interest: anterior occipital (*Oy*), anterior parietal (*Ps*), midline precentral (superior edge-*Cs*), and midline premotor (*Csa*) areas. (B) Composite average event-related potentials (ERP's) from four persons (75 percent of the total data from nine persons) for the Pz electrode, showing the major ERP peaks and corresponding single trial correlation analysis intervals. The P300 ERP peak is larger in the infrequent no-move trials. (C) One of the 15 sets of ten electrode pairs into which the 91 paired correlations were grouped. The anterior occipital (*Oy*) set is shown. In Fig. 2 the principal electrodes of differing sets are circled and the most prominent correlations are indicated as solid and dotted lines.

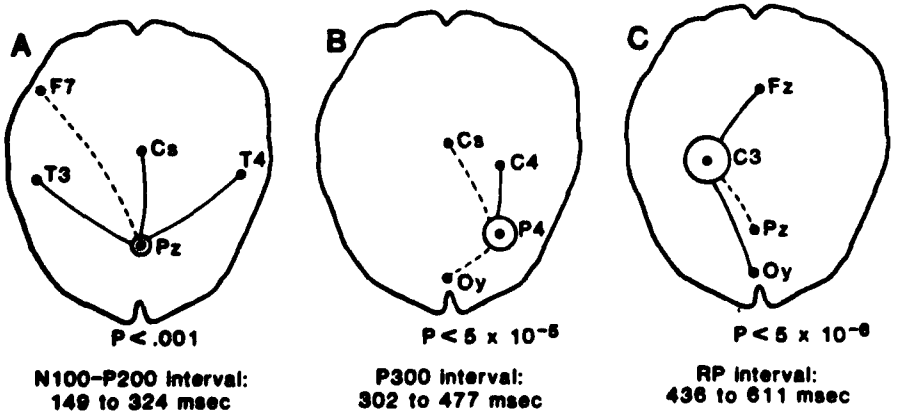

Fig. 2. Diagrams of between-task differences in the (A) N100–P200, (B) P300, and (C) RP intervals generated by neurocognitive pattern (NCP) analysis. The most significantly differing electrode sets, their significance level, and the most prominent correlations within the set are shown. A solid line between two electrodes indicates that the correlations were higher in the move task, while a dotted line indicates higher no-move task correlations.

is not clear whether this activity is associated with mental aspects of tasks or with sensorimotor components, or with artifacts. In a previous study we found no topographic differences in EEG spectra between 15-second arithmetic, block rotation and letter substitution tasks after rigorously controlling other-than-cognitive factors (*2–4*). However, such heterogeneous tasks cannot be resolved into serial components reflecting different neurocognitive processes. We therefore refined our approach by using short (less than 1 second) tasks, using time references based on person-specific average ERP measurements, computing correlations between channels on a single-trial basis, and using mathematical pattern classification to reveal split-second sequential processing. This yielded a sequence of clear-cut between-task difference patterns involving split-second changes in the localization and lateralization of mass neural activity. Appropriate studies of neurocognitive functions should take into account this rapidly shifting network of localized and lateralized processes.

ALAN S. GEVINS
ROBERT E. SCHAFFER
JOSEPH C. DOYLE
BRIAN A. CUTILLO
ROBERT S. TANNEHILL
STEVEN L. BRESSLER

EEG Systems Laboratory,
1855 Folsom Street,
San Francisco, California 94103

References and Notes

1. E. Donchin, M. Kutas, G. McCarthy, in *Lateralization in the Nervous System*, S. Harnard *et al.*, Eds. (Academic Press, New York, 1977), pp. 339–384.
2. A. Gevins, G. Zeitlin, C. Yingling, J. Doyle, M. Dedon, R. Schaffer, J. Roumasset, C. Yeager, *Electroencephalog. Clin. Neurophysiol.* **47**, 693 (1979).
3. A. S. Gevins, G. M. Zeitlin, J. C. Doyle, C. D. Yingling, R. E. Schaffer, E. Callaway, C. L. Yeager, *Science* **203**, 665 (1979).
4. A. Gevins and R. Schaffer, *CRC Crit. Rev. Bioeng.* **1980**, 113 (1980).
5. A. S. Gevins, J. C. Doyle, R. E. Schaffer, E. Callaway, C. Yeager, *Science* **207**, 1006 (1980).
6. A. Gevins, in *Cerebral Hemisphere Asymmetry: Method, Theory and Application*, J. Hellige, Ed. (Praeger, New York, in press).
7. D. Friedman, R. Simpson, W. Ritter, I. Rapin, *Electroencephalog. Clin. Neurophysiol.* **38**, 13 (1975); C. Wood, *J. Exp. Psychol. Hum. Percep.* **104** (No. 1), 3 (1975); J. Marsh and W. Brown, *Prog. Clin. Neurophysiol.* **3**, 60 (1977); R. Thatcher, *Behav. Biol.* **19**, 1 (1977).
8. J. Hellige, Ed., *Cerebral Hemisphere Asymmetry: Method, Theory and Application* (Praeger, New York, in press).
9. M. Livanov, *Spatial Organization of Cerebral Processes* (Wiley, New York, 1977); J. Busk and G. Galbraith, *Electroencephalog. Clin. Neurophysiol.* **38**, 415 (1975); E. Callaway and P. R. Harris, *Science* **183**, 873 (1974).
10. A. Gevins, *IEEE Trans. Patt. Anal. Machine Intell.* **2**, 383 (1980); S. Viglione, in *Adaptive Learning and Pattern Recognition Systems*, J. Mendel and K. Fu, Eds. (Academic Press, New York, 1970), pp. 115–163.
11. The two-layered, nonlinear, distribution-independent trainable classification-network algorithm used in this study is described in A. Gevins, J. Doyle, R. Schaffer, B. Cutillo, R. Tannehill, S. Bressler, *Electroencephalog. Clin. Neurophysiol.*, in preparation; and Gevins *et al.* (*12*).
12. A. Gevins, J. Doyle, G. Zeitlin, S. Bressler, *IEEE Trans. Patt. Anal. Machine Intell.*, in preparation.
13. A. S. Gevins, J. C. Doyle, B. A. Cutillo, R. E. Schaffer, R. S. Tannehill, J. H. Ghannam, V. A. Gilcrease, C. L. Yeager, *Science* **213**, 918 (1981). In the key for figure 3 of that report, $P < .005$ should have been next to the blank circle, while $P < .5 \times 10^{-5}$ should have been next to the hatched circle.
14. The stimulus subtended a visual angle of less than 2 degrees. The vertical position and side of screen of the target changed randomly across trials for both tasks, as did the horizontal angle and direction of the arrow. Response was made on a Grass isometric force transducer and varied randomly across trials from 0.1 to 1 kg. An individual trial consisted of a neutral warning that was followed after 2 seconds by the stimulus. One second after its completion the response was displayed.
15. Brain potentials were amplified with a Bioelectric Systems model AS-64P and Beckman Accutraces with a passband of about 0.1 to 50 Hz. Electroculogram and muscle potentials were amplified by a Grass model 6 with similar filter settings. All signals were digitized to 11 bits at 128 samples per second, and a 12-Hz, 15-point nonrecursive digital low-pass filter was applied.
16. A task-by-electrode-by-person analysis of variance of the P300 peak voltage revealed a significant task effect [$F(1, 8) = 29.0$, $P < .001$] and task-by-electrode interaction [$F(13, 104) = 2.9$, $P < .005$]. Correlated t-tests revealed P300 voltage enhancements in the no-move task for all but the lateral temporal electrodes; the most significant difference ($P < .0005$) was at the anterior midline parietal electrode. When corrected for multiple comparisons by the Bonferroni method only the right central, anterior, and posterior midline parietal electrodes reached significance ($P < .05$). P300 ERP peak amplitude increases have been associated with similar go versus no-go decisions [R. Simson, H. Vaughan, W. Ritter, *Electroencephalog. Clin. Neurophysiol* **43**, 864 (1977)] and with the perception of a novel or relevant stimulus. This study differs from typical P300 studies in that a difficult motor response is required to the more frequent stimulus.
17. A task-by-electrode-by-person analysis of variance of the slope of a straight line fitted to the slow-potential shift across the RP interval revealed a significant task effect [$F(1, 8) = 5.6$, $P < .05$], electrode effect [$F(14, 112) = 1.9$, $P < .05$], and task-by-electrode interaction [$F(14, 112) = 2.7$, $P < .005$]. Correlated t-tests showed larger move task slopes for nine electrodes; the most significant difference ($P < .005$) was at the left central electrode. When Bonferroni-corrected, no electrode reached significance at $P < .05$.
18. The N100–P200 and P300 centerpoints in milliseconds for each of the volunteers were: V1 (218, 452); V2 (200, 388); V3 (228, 482), V4 (210, 462); V5 (203, 398); V6 (208, 298); V7 (212, 368); V8 (181, 318); and V9 (203, 358). The RP interval was centered 135 msec after the P300 centerpoint.
19. The functions were derived from two-thirds of the data and were tested on the remaining one-third. This was repeated three times and the average test-set classification accuracy was computed. A test-set classification accuracy of 55 percent corresponds to $P < 5 \times 10^{-4}$. This is more than 3.8 standard deviations above the mean classification accuracy of 48 classifications using 1612 randomly labeled move and no-move trials. Mean accuracy on the randomly labeled data was 50.6 percent, with a standard deviation of 1.1 percent, an accuracy that could have occurred by chance with $P = .32$ according to the binomial distribution. High classification accuracy was not the objective. Rather, the relative classification accuracy of each electrode set was used as an indicator of anatomic and temporal localization of task-related patterns. The classification accuracy of the P300 and RP intervals assessed on each individual was at the chance level for only two of the nine people. Their data comprised only 9 percent of the total data set. When the entire analysis was performed on the data of one person (V7) in the P300 interval, the P4 electrode set again achieved the highest classification accuracy.
20. To select the most prominent correlations from significant classification functions, the pattern recognition analysis was applied recursively on the highest weighted correlations. Test-set classification accuracy based on the final three or four correlations was significant at $P < .001$ or better in each interval.
21. The P300 ERP peak has not been found to vary in lateralization specifically as a function of cognitive task (*1*). J. Desmedt [*Proc. Natl. Acad. Sci. U.S.A.* **74**, 4037 (1977)] reported a qualitative change in the ERP over the right hemisphere in a somatosensory-motor task, but the effect was general and was not present in the P300 peak.
22. We thank the late Gobind B. Lal for the "shadows of thought" metaphor; H. Currens for manuscript preparation and artwork; G. Gilcrease and J. Ghannam for assistance with recordings and analysis; R. Adey, M. Aminoff, P. Bach-y-Rita, F. Benson, E. Callaway, J. Engel, B. Garoutte, W. Gersch, R. Halliday, E. Roy John, B. Libet, J. Mazziotta, M. Mesulam, K. Pribram, J. Roumasset, A. Salamy, C. Skomer, J. Spire, H. Vaughan, D. O. Walter, C. Woods, and J. Vidal for valuable comments; J. Miller (Air Force School of Aerospace Medicine), D. Woodward (Office of Naval Research), A. Fregly (Air Force Office of Scientific Research), J. Fetzer, and M. Bachman-Hoffman for research support.

19 November 1982; revised 1 February 1983

NOTE 18a. The average ERP waveforms (Figure 1B) contain several late positive peaks. P391 and P530 are larger in amplitude in the infrequent no-move trials, while P425 is larger in the frequent move tirals. The P300 analysis interval was centered on P391, the earliest positive peak to show a significant between-task difference maximal at the anterior midline parietal electrode ($p<.0005$). Since P391 and P530 were larger in the infrequent no move trials, and P391 followed a negative difference ERP peak (N2) at 240 msec, P391 and P530 could be designated P3a and P3b according to the convention of Squires, et al (Electroenceph. Clin. Neurophysiol. 38;387-401, 1975). The P300 interval might then be specified as the "P3a interval", as in our previous study of similar tasks (Gevins, et al, Science, 213:918-922, 1981). The response preparation (RP) interval, centered 135 msec after the P300 interval, also spans the P530 peak of the no-move trials.

Section IV

NEUROCOGNITIVE PATTERN ANALYSIS OF A VISUOMOTOR TASK: LOW-FREQUENCY EVOKED CORRELATIONS

Alan S. Gevins, Joseph C. Doyle, Brian A. Cutillo, Robert E. Schaffer, Robert S. Tannehill, Steven L. Bressler,

EEG SYSTEMS LABORATORY
1855 Folsom
San Francisco, CA 94103
415-621-8343

Note to colleagues: This manuscript has been submitted for publication. We would appreciate receiving your cricital comments and suggestions. Thanks.

ABSTRACT

Spatial patterns of single-trial evoked correlations of human scalp-recorded brain potentials were determined by applying Neurocognitive Pattern (NCP) analysis to data from nine adults performing a visuospatial task. Mathematical pattern recognition was used to determine the differences in the spatial patterns of correlation of "move" and "no-move" trials in successive 175-msec intervals. The magnitude of the patterns of difference between tasks increased in each successive interval. In the prestimulus interval, correlation of the midline frontal electrode with lateral central and left temporal electrodes was greater for the no-move task, while its correlation with the left parietal electrode was greater for the move task ($p<.01$). In the interval spanning the N1, P2 and N2 event-related potential (ERP) peaks, the between-task contrast was focused at the midline parietal electrode and involved higher correlation of that electrode with lateral temporal and midline precentral electrodes in the move task, and with the left frontal (F7) electrode in the no-move task ($p<.001$). In the interval centered on the P3a peak, the focus of correlation difference was at the right parietal electrode and involved higher correlation of the right parietal with occipital and midline precentral electrodes in the no-move task, and with the right central electrode in the move task ($p<5\times10^{-5}$). In the interval centered 135 msec after the P3a ERP peak, and which included the right-handed response preparation and initiation, the major focus of contrast shifted to the left central electrode, involving higher correlation of that electrode with midline frontal and occipital electrodes in the move task, and with the midline parietal electrode in the no-move task ($p<5\times10^{-6}$). In seven of the nine participants, the group equations significantly distinguished the tasks. Move and no-move trials which were behaviorally correct, but which were misclassified by the algorithm showed high prestimulus alpha activity in the averages, and had post-stimulus waveform morphologies intermediate between correctly classified move and no-move types. Although the neurophysiological significance of these patterns of evoked correlation is unknown, the results are consistent with the observation in humans and primates that simple visuospatial tasks involve the integration of spatially-distributed activity in many neural areas.

INTRODUCTION

Neurocognitive Pattern (NCP) analysis is a method of measuring the functional topography of human scalp-recorded brain potentials during goal directed activity. It involves application of mathematical pattern recognition to measures of inter-electrode correlations of single-trial evoked brain potentials. Here we report the measurement of rapidly shifting, focal patterns of correlation which distinguish two variants of a brief 'move/no-move' visuospatial task.

It has been proposed that task-specific neural processes manifest patterns of waveshape similarity (crosscorrelation) of low-frequency macropotentials (Dumenko, 1970; Livanov, 1977). A number of studies have approached this issue with scalp-recorded EEGs (Walter and Shipton, 1951; Brazier and Casby, 1952; Callaway and Harris, 1974; Busk and Galbraith, 1975; Livanov, 1977), but this hypothesis remains unproven due to problems of experimental design and lack of methodology for precise measurement of task-related correlation patterns at the scalp.

Any test of the hypothesis that waveshape similarity among scalp-recorded brain potentials reflects task-related processing in underlying neural populations must meet several methodological criteria. First, the functional relationships of specific areas must be explicitly manipulated. Well established 'landmarks' such as sensory, 'association' and motor areas must be used as anatomic reference points in the experimental design, and the scalp projections of the presumed generators must be considered. Second, the experiment must be rigorously controlled for stimulus, cognitive, performance and response-related factors to allow unambiguous association of experimental manipulations with spatiotemporal electrical patterns. Third, a high degree of temporal resolution is required, since the neural processes involved in brief cognitive tasks last only a fraction of a second. Fourth, measures must be made on single-trial EEG timeseries rather than averages, since the exact timing of neurocognitive processes may vary from trial to trial. Fifth, the analytic method must be able to extract small task-related signals from the obscuring effects of background activity and volume conduction.

Our first study employing NCP analysis (Gevins, et al, 1981) revealed complex, rapidly changing patterns of evoked correlation which involved many areas of both hemispheres which differed between numeric and spatial judgments performed on equivalent stimuli. However, the complex patterns were difficult to interpret since the sequencing of neurocognitive activity in numeric and spatial judgments is not definitively known. The present study was designed to clarify this situation by highlighting presumably localized neural processes. In comparing the move and no-move variants of a spatial judgment task the common activity of brain areas should cancel, revealing focal differences in visual and parietal areas presumed to mediate visual discrimination and spatial judgments. The

right-handed response in the "move" task should elicit lateralized activity of the left central motor area.

METHODS

Tasks and Protocol

The participant (P) was seated in an acoustically dampened recording chamber with right-hand index finger resting on a force transducer. Stimuli were presented on a Tektronix graphics terminal and subtended a visual angle of less than 2 degrees horizontally and vertically. They consisted of an arrow originating at center screen and a vertical line segment (the "target") to one side (Fig. 1). The target's vertical position and side of screen changed randomly across both move and no-move trials, as did the angle and direction of the arrow. The arrow's angle varied from 0 to 30 degrees from the horizontal, and target size ranged from 2 to 36 mm (see below). Stimuli remained on the screen until feedback was presented. On move trials the participant was to estimate the distance the target must be moved so that the arrow's trajectory would intersect its center, and apply a pressure proportional to that distance with a ballistic contraction of the right index finger. Responses were made on a Grass isometric force transducer with maximum 1mm travel at a force rate of 1 kg/mm. The required force varied randomly from .1 to 1 kg. On "no-move" trials the arrow and target were oriented so that the arrow's trajectory would intersect the center of the target, and no movement was to be made (Fig. 1).

Trials occurred in blocks of 13 or 17. The blocks were self-initiated by the participant and lasted about 1.5 min. The no-move trials constituted 20% of the total number of trials and were presented in semi-random order such that the first two trials of a block were always move trials, and a no-move trial was always followed by a move trial. Each trial consisted of a warning symbol followed after 2 sec by the stimulus. One second after completion of response in the move task, feedback indicating the response pressure was presented for 1 sec. Feedback for no-move trials was presented 3.5 sec. post-stimulus. The inter-trial interval was 1.8 sec.

Two factors were included to reduce the automatization of task performance. First, at the start of each block of trials the gain of the response transducer was switched between 2 levels of sensitivity, requiring the participant to adjust his responses between 2 pressure/distance scales. Second, the target automatically shrank or lengthened (from 2 to 36 mm) for both move and no-move trials as an on-line function of accuracy in the previous 5 move trials. Thus task difficulty was continually adjusted to match each person's current performance level.

Recordings

Nine right-handed adults (8M, 1F) were recorded. The first five were healthy students and professionals, ages 20 to 35, who received about

50 practice trials before performing the tasks during 2.5 hour recording sessions. The last four were highly skilled aircraft pilots who had several hundred practice trials and who performed a large number of trials in 6 hour recording sessions.

Brain potentials were recorded from 15 scalp electrodes and referenced to linked mastoids (Fig. 2a). The montage included several non-standard midline placements intended to overlie cortical areas of particular interest: 'aOz' (anterior occipital), 'aPz' (anterior parietal), 'aCz' (precentral), and 'pFz' (anterior motor). The first five Ps' brain potentials were amplified by two Beckman Accutraces with .16 to 50 Hz passband; for the other four a Bioelectric Systems Model AS-64P amplifier with .10 to 50 Hz passband was used. Vertical and horizontal eye-movement potentials (electrodes at outer canthi and above and below one orbit), response-muscle potentials (flexor digitorum), and response transducer output were amplified by a Grass Model 6 with .30 to 70 Hz passband. All signals were low-pass filtered at 50 Hz (40 dB/octave rolloff) and digitized to 11 bits at 128 samples/sec.

Software System

The ADIEEG, integrated software system, was used for all aspects of the experiment (Gevins and Yeager, 1972; Gevins, et al, 1975, 1979a, 1981, 1983b). This system performs real-time control of experiments and behavioral and physiological data collection; allows automatic on-line modification of experimental parameters as a function of task performance; has a flexible database structure and integrated data path for the recording and analysis of up to 56 physiological channels; allows selection and control of the stimulus, response and performance-related variables used to aggregate trials into data sets; performs digital filtering and timeseries analysis of EEGs and ERPs; and tests hypotheses with linear univariate and multivariate analyses and mathematical pattern recognition.

Formation of Data Sets

Polygraph records were edited off-line to eliminate trials with evidence of eye movement in the EOG channels, or muscle or instrumental artifacts in the EEG channels, from 0.5 sec before the stimulus to 0.5 sec after response initiation. The total set of 1612 trials (839 move, 773 no-move) submitted to analysis consisted of 69 to 350 behaviorally correct trials from each of the 9 participants (Table 1). Correct move trials were those in which the participant's response was ballistic, was completed by 1.5 sec after stimulus onset, and was not greatly 'off target'. Correct no-move trials were those in which no EMG was evident in response to the 'no-move' stimulus configurations. There was no difference between the two data sets in the stimulus parameters of arrow angle and side of screen of the arrow and target, since these parameters were randomized by the program. Target size was balanced between move and no-move trials. The set of move trials had representative distributions of response variables including response initiation time, accuracy, pressure, duration, and velocity. Response initiation was determined by the

beginning of the average EMG burst of the right index finger's flexor digitorum. Thus move and no-move tasks differed slightly in expectancy and stimulus configuration, differed in the decision based on spatial judgment, and differed greatly in type and difficulty of response.

Average ERPs

Average ERPs for all channels were computed for each person in order to determine centerpoints of time intervals for NCP analysis. Amplitudes of the major ERP peaks were measured from a 500-msec prestimulus baseline. N1 was the first major negative deflection, maximal posteriorly. P2 was the immediately succeeding positive deflection, maximal at the anterior parietal electrode. P3a and P3b were the first and second positive peaks enhanced in the infrequent no-move task and maximal at parietal electrodes. The immediately succeeding negative potential shift (in the move trials) was measured as the slope of a straight line fitted to the ERP in the 175-msec interval centered 135 msec after the P3a peak.

Single Evoked Trial Correlations

After applying a phase-preserving, nonrecursive digital lowpass filter (3 dB amplitude point at 12 Hz) to the single-trial timeseries, crosscorrelations between pairs of electrodes were computed according to the formula:

$$\frac{N \sum XY - \sum X \sum Y}{N^2 \, s_x \, s_y}$$

where X and Y are the sampled voltages of channels x and y at N time points, and s_x, s_y their standard deviations. A Fisher's z' transformation was then applied to each correlation value. Correlations were computed for each of the 1612 trials in each of 4 analysis intervals for 91 of the 105 possible pairwise combinations of electrodes (Fig. 2b). 14 pairs which were non-homologous or closely spaced were excluded due to computational limitations.

Since the major ERP peaks indicate the average latencies of distinct task-related processes, the centerpoint locations of three of the four 175 msec analysis intervals were determined from the peak latencies of the average ERP (Fig. 3). This was done separately for each person to account for individual variations. The first interval was the 175 msec epoch preceding the stimulus. The second interval straddled each person's N1-P2 peak complex, and the third was centered on the P3a peak, which was the first positive peak to show a between task difference. The fourth interval was centered 135 msec after the P3a peak and spanned a portion of the response preparation (RP) in the move trials and the P3b peak in the no-move trials. (An NCP analysis synchronized to the movement onset will be reported elsewhere).

To equalize the scale of correlation values across people, the Fisher z'-transformed correlations were converted to standard scores within each person's data in each interval (x=0, s=1) and then grouped across people. ANOVAs and t-tests were performed on the single-trial correlations to determine task-related differences observable by linear statistical methods.

Use of Mathematical Pattern Recognition for Spatiotemporal Analysis

The analysis of between-task differences in spatial patterns of evoked correlation was performed with nonlinear, distribution-independent, trainable classification-network mathematical pattern recognition (Viglione, 1970; Gevins, 1980; Gevins, et al, 1979a, 1981, 1983ab). This method is similar in purpose to stepwise discriminant analysis, but uses a more sophisticated algorithm to search for combinations of variables which distinguish the data of two conditions of an experiment. The search is conducted on a task-labeled portion of the data, called the training set, and then the extracted patterns of difference (classification equations) are verified on the remaining unlabeled data, called the test set. If these classification equations can significantly divide the test set into the two conditions, the extracted patterns can be said to have intrinsic validity.

To avoid spurious results, the sensitivity of this method requires that the experimental conditions be highly balanced for all factors not related to the intended manipulations (Gevins and Schaffer, 1980; Gevins, et al, 1980, 1983b; Gevins 1980; 1983ab), and that the ratio of observations to variables be on the order of 20 to 1 or more. The variables submitted to analysis should be grouped (constrained) according to neuroanatomical and neurophysiological criteria so that interpretable results may be obtained (Gevins, et al, 1979ac, 1981, 1983ab; Gevins 1980). In this study temporal constraints consisted of locating the analysis intervals according to the major peaks of each person's average ERP. Anatomical constraints were applied by forming sets consisting of the correlations of each of the 15 scalp electrodes (called a principal electrode) with 10 other electrodes (Fig. 2c). (To reduce the amount of computation, 4 of the 14 possible pairings were excluded from each set. These involved electrodes adjacent to the principal electrode, or pairings nearly redundant with others.) Midline sets were symmetrical, and lateral sets were mirror images of each other.

Classification equations. A separate classification equation was computed for each of the 15 electrode sets in each analysis interval for each task-labeled training set. Each classification equation consisted of a linear combination of the binary decisions of 1 to 6 discriminant functions. Each discriminant function consisted of a linear combination of 6 correlations selected by the algorithm from the 10 electrode-pair correlations of an electrode set.

A recursive procedure was used to develop each classification equation. First, 15 discriminant functions were computed (this number was set by computer limitations), and the best was retained as a binary output (move or no-move) times a coefficient weighted for optimum classification performance by minimization of an exponential loss function. This process was repeated 6 times; the best discriminant function from each new set of 15 was added to the evolving classification equation, and the weights assigned to each were updated. After each pass, the training data were re-weighted inversely to the classification effectiveness of the classification equation, so that the next pass would concentrate on the incorrectly classified data. In this way a classification equation which optimally partitioned the training data set into move and no-move tasks was formed.

Training and testing (validation) data sets. The data set of 1612 trials was partitioned into 3 non-overlapping test (validation) sets. For each test set, the remaining two-thirds of the data served as its training set. This rotation of training and testing sets reduced sampling error due to test-set selection.

A separate classification equation was formed using each of the 3 training sets. Then the classification accuracy of each of the 3 equations for each interval was measured on its corresponding test set, and the average test-set classification accuracy was determined.

Significance levels of classification. Since our aim was to determine task-related spatiotemporal patterns, rather than to predict behavior, the analysis was constrained to facilitate a neuroanatomically and neurophysiologically meaningful interpretation. Thus classification accuracies were not as high as they would have been without constraints. To determine the significance levels of the classification accuracies it was necessary to determine a baseline significance level and safeguard against a Type 1 error. To do this, equations were formed from sets of randomly task-labeled data for each analysis interval. The average classification accuracy of 48 such random-labeled studies was 50.6%, with a standard deviation of 1.1%. This could have occurred by chance with $p=.32$, according to the normal-curve approximation to the binomial distribution. Actual test-set classification accuracies of 52.9%, 53.9%, 54.9% and 55.5% correspond to $p<.01$, $p<.001$, $p<5 \times 10^{-5}$ and $p<5 \times 10^{-6}$, respectively. These significance levels were used as an index of the relative consistency of differences between move and no-move tasks.

Diagrams of classification equations. In order to illustrate the strongest between-task differences, diagrams were drawn showing the principal electrode and the electrode pairings which contributed most to the classification function for the most significant electrode set in each interval. These "prominent" evoked correlations were determined by applying the pattern recognition procedure recursively to the most significant electrode set. Each discriminant function (combination of correlations) whose weight was more than 0.1 times that of the maximum weighted function was retained on each pass.

Within the selected discriminant functions, those correlations whose weight was more than .25 times the highest weighted correlation were retained. The selected correlations were weighted by the number of discriminant functions remaining in the classification equation, and summed over the 3 test sets. The 5 highest weighted correlations were then input to the pattern classifier. If 'test-set' classification for a given interval was still significant at $p<.01$, the entire procedure was repeated with the least significant correlation removed until a classification function incorporating a minimum set of 3 or 4 'prominent correlations' was produced.

RESULTS

Average ERP Description

The average ERP waveforms from Ps #6-9 (Fig. 4) consisted of a posteriorly maximum negative peak (N163) and a centro-parietally maximum positive peak (P230) in both tasks. In the move task there were parietally maximum positive peaks at 425 and 500 msec, followed by a centrally maximum, left-lateralized negative-going slow potential shift. In the no-move task a positive peak was observed at 391 msec, maximal at the anterior parietal electrode (aPz), another at 425 msec and a third at 530 msec, both maximal at the midline parietal electrode (Pz). Subtraction ERPs (Fig. 5) showed that the P391 peak in the infrequent no-move task immediately follows a negative peak (N2) at 240 msec, and thus may be the probability sensitive P3a peak (Squires, et al, 1977). The larger amplitude of P425 in the move task may be due to the atypical experimental paradigm, in which a difficult response is required to the frequent task-related stimuli. P530 in the infrequent no-move task may correspond to the P3b peak observed in go/no-go paradigms and to infrequent task-related stimuli. Peak latencies, the corresponding NCP analysis intervals, and response initiation times for each person are given in Table 1.

ANOVAs and t-tests were performed for the P391 (P3a) peak amplitude and the slope of the immediately succeeding slow negative potential shift. For the P391 peak, a task x electrode x person ANOVA revealed a significant task effect ($F(1,8) = 29.0$, $p<<.001$) and task x electrode interaction ($F(13,104) = 2.9$, $p<.005$), but no electrode effect ($F(13,104) = 1.2$, N.S.). Correlated t-tests revealed significant voltage enhancements in the no-move task for all but the lateral temporal electrodes, the most significant effect being at the midline anterior parietal electrode (aPz) ($p<.0005$) (Table 2). When Bonferroni-corrected for multiple comparisons, only the aPz, Pz and C4 electrodes remained significant ($t = 4.35$ for $p<.05$). Mean amplitudes across persons at aPz were .1 uV and 2.3 uV for move and no-move tasks, respectively.

A task x electrode x person ANOVA of the slope of a straight line fitted to the slow potential shift in the response preparation (RP) interval revealed a significant task effect ($F(1,8) = 5.6$, $p<.05$), electrode effect ($F(14,112) = 1.9$, $p<.05$), and task x electrode

interaction ($F(14, 112) = 2.7$, $p<.005$). Correlated t-tests showed significantly larger move-task slopes for 9 electrodes (Table 3). The most significant difference ($p<.005$) was at the C3 electrode, where the mean slope values were .24 and -.50 for move and no-move tasks, respectively. When Bonferroni-corrected for multiple comparisons, no electrode remained significant ($t = 4.35$ for $p<.05$).

Linear Analysis of Evoked Correlations

Mean evoked correlation values over persons and electrode pairs were, for the move trials: prestimulus interval = .64, N1-P2 interval = .65, P3a interval = .65, RP interval = .65; and for the no-move trials: prestimulus = .65, N1-P2 = .65, P3a = .65, and RP = .64. t-tests of differences in single-trial correlations between tasks were performed for the 91 electrode-pair correlations (Table 4). When Bonferroni-corrected for multiple comparisons only the F7-T3 and F8-Pz pairs in the RP interval reached significance ($t= 3.58$ for $p<.05$). Without Bonferroni correction, correlations significant at $p<.05$ or better were found in every interval. In the prestimulus interval 5 of the 9 significant electrode pairs included the Fz electrode. In the N1-P2 interval the 4 significant pairs all included parietal sites. In the P3a interval the 6 significant pairs were fronto-central, with the exception of the P4-C4 pair. In the RP interval the 25 significant pairs were widely distributed, but 8 included Fz, 9 included F8, and 5 included C3.

Pattern Recognition Analysis of Single-Trial Evoked Correlations

Pattern recognition analysis revealed patterns of difference in evoked correlation which increased in magnitude in each successive interval. The principal electrode and prominent correlations of the most significant electrode set in each interval are shown in Figure 6. In the prestimulus interval there was a weak between-task difference of the Fz electrode set ($p<.01$), involving higher prominent correlations of Fz with P3 in the move task and higher correlations of Fz with T3, C3 and C4 in the no-move task.

In the N1-P2 interval the distinguishing significant difference was in the Pz electrode set ($p<.001$), with higher correlations of Pz with aCz, T3 and T4 in the move task, and higher correlations of Pz with F7 in the no-move task.

In the P3a interval the most significant difference was in the P4 electrode set ($p<5 \times 10^{-5}$), with higher correlations of P4 with C4 in the move task, and higher correlations of P4 with aCz and aOz in the no-move task. At the $p<.001$ level the aOz electrode set also distinguished the tasks.

In the RP interval the most significant difference was in the C3 electrode set ($p<5 \times 10^{-6}$), with higher correlations of C3 with Fz and aOz in the move task, and higher correlations of C3 with Pz in the no-move task. Four other electrode sets distinguished the tasks at lower significance levels: C4 ($p<1 \times 10^{-5}$), F7 and T3 ($p<5 \times 10^{-4}$), and Pz ($p<.001$).

For the prestimulus and N1-P2 intervals the reduced classification functions required 4 "prominent correlations" to achieve significant classification, while in the P3a and RP intervals only 3 were needed. Further, significant classification ($p<.05$) could be achieved with just the first term (discriminant function) of the reduced classification equation (Table 5).

To test the interperson validity of the results, the classification accuracies of the classification equations for the P4 electrode set in the P3a interval and the C3 set in the RP interval were assessed on the data of each person individually, and compared with the overall classification accuracy (Table 6). The group equations were valid for 7 of the 9 people. As a further test, the entire analysis was performed on the data of one person (255 trials from P #7) for the P3a interval. The P4 electrode set again achieved the highest classification accuracy (59.4%; $p<5 \times 10^{-3}$).

DISCUSSION

Neurophysiological Significance of Task-Related Evoked Correlations

In theory, a task-related difference in evoked correlation between two scalp electrodes could be due to one or more possible causes: 1) functional coordination of two distinct cortical populations, 2) driving by a third cortical or subcortical neural area, and 3) volume conducted activity from a distant generator. While it is if the task-related patterns of evoked correlation determined by Neurocognitive Pattern (NCP) analysis reflect functional coordination between cortical (and possibly subcortical) areas, their anatomical and temporal specificity suggests that significant aspects of task-related neural processes are being measured. (A preliminary NCP Analysis of single channel signal power determined significant, but weaker, between-task patterns of difference. Some of the significant electrodes corresponded to those found with correlation measures. These results will be reported elsewhere.) However, the significance of waveshape similarity in scalp-recorded brain potentials will not be understood until further studies are completed.

NCP Analysis, ERPs and Neuropsychology

In this section the main NCP results will be discussed in light of previous neuropsychological and electrophysiological (ERP) findings, showing how they concur with and elaborate the information obtainable by those methods. Psychological interpretation of these results must be considered speculative, since the processing stages involved in the task are not definitively known.

The magnitude of between-task difference increased from interval to interval. The presence of a small significant effect in the prestimulus interval might be the result of a weak task-specific preparatory set generated in the course of the session by the ordering of move and no-move trials. The locus of this difference in the Fz electrode set is consistent with neuropsychological and

electrophysiological (CNV) findings suggesting involvement of prefrontal cortex in preparatory activity (Teuber, 1964; Walter, 1967; Fuster, 1980). A previous NCP study (Gevins, et al, 1981) also revealed evidence of a task-specific preparatory set in the task-cued prestimulus interval preceding numeric and spatial judgments. The prominent correlations of Fz with T3, C3, C4 and P3 in the present study suggest that this preparatory activity extends beyond prefrontal areas.

In the N1-P2 interval, correlations of the Pz electrode set distinguished move and no-move tasks at $p<.001$. Subtraction ERPs revealed an enhancement of the N2 peak no-move trials in 6 of the 9 participants (79% of the total data set) (Fig. 5). Its mean latency of 240 msec. placed it near the center of the N1-P2 analysis interval, and its amplitude was maximal (1.7 uv) at Pz. Thus the between-task correlation differences in this interval may be related to N2. Although an amplitude increase in the N2 peak in no-go trials of a go/no-go paradigm with equiprobable conditions has been reported (Simson, et al, 1977), N2 has usually been reported to be sensitive to infrequent changes in gross stimulus properties or patterns (Naatanen, et al, 1980). However, in the present study, stimuli were equivalent between conditions in all respects, save that in no-move trials the arrow pointed directly at the target in various randomly-ordered configurations. The N2 effect at 240 msec suggests that a no-move configuration has been identified by that time, and that N2 may reflect a more subtle process than the detection of a gross "mismatch" in stimulus characteristics, as indicated by other recent studies (Ritter, et al, 1982). The prominent correlations of Pz with T3, F7, aCz, and T4 suggest that these processes are not confined to the parietal area.

In the P3a interval (which was centered on the P3a peak and overlapped a portion of the P3b peak) the right parietal (P4) locus of correlation differences ($p<5 \times 10^{-5}$) provides novel evidence for the lateralization of neural processes related to these late positive ERP peaks. Although on the basis of lesion evidence, the right parietal cortex is known to be necessary for such spatial judgments, the late positive ERP peaks have not been found to vary in lateralization according to type of cognitive task (Donchin, et al, 1977). J. Desmedt (1977) reported a relative right-sided lateralization in the ERP in a spatial somatosensory-motor task, but the effect was general and was not present in the P3 peak, nor was its scalp distribution determined. A previous NCP study (Gevins, et al, 1981) demonstrated lateralized temporo-parietal evoked correlation differences between numeric and spatial judgments in the interval centered on the P3a peak at 340 msec., but the interval centered on the P3b peak at 450 msec. exhibited bilateral between-task differences from frontal, central, and parietal electrodes. In the present study, the between-task differences in correlations of the right parietal electrode with central and occipital electrodes is in accord with neuropsychological expectations, as is the somewhat weaker effect in the aOz electrode set. The lateralized NCP finding is in contrast with the anterior midline parietal (aPz) locus of maximal amplitude difference of the

P3a ERP peak.

In the response preparation (RP) interval, centered 135 msec after the P3a interval centerpoint, the focus of between-task difference shifted to the left central (C3) electrode set ($p<5 \times 10^{-6}$), involving higher correlations of C3 with Fz and aOz in the move task and with Pz in the no-move task. Since the RP interval overlapped EMG onset in a portion of the set of move trials (average response time = 590 msec, mean S.D. within persons = 240 msec.), the RP interval results may also include a contribution from the output activity of motor cortex. The C4, F7, and T3 electrode sets, which differed at lower significance levels, may also reflect movement preparation and initiation, since the presumed generators of voluntary finger movements are buried in the lateral bank of the central sulcus and their scalp projection may be diffuse. The less significant difference in the Pz electrode set may reflect concurrent processes related to P3b.

Rapidly Shifting Lateralization

The rapid (135 msec) shift in side and site of lateralization from the P3a to the RP interval may help clarify the controversy surrounding the existence of lateralization of brain potentials in different types of cognitive activity. Although various 'verbal-analytic' and 'spatial' tasks lasting one minute or more have been associated with relative left and right hemisphere activity, it is not clear whether this is due to cognitive activity, or to stimulus, motor, or arousal-related aspects of the tasks (Donchin, et al, 1977; Gevins and Schaffer, 1980; Gevins, et al, 1980; Gevins, 1983ab). In an earlier study (Gevins, et al, 1979abc), we first found prominent spatial differences, including lateralized patterning of EEG spectra, between one minute linguistic and spatial tasks (reading and writing, Koh's Block Design and mental cube reconstruction). However, no spatial differences in EEG spectra were found between similar 15 second tasks which were more controlled for other-than-cognitive factors. Since heterogeneous tasks composed of many component operations cannot be clearly resolved into serial processes, our subsequent study (Gevins, et al, 1981) refined the approach. It used short (less than 1 second) visuomotor tasks differing only in type of judgment (numeric and spatial), employed 175-msec analysis intervals based on person-specific ERP measurements, and used measures of between-channel correlations in single trials as features for NCP Analysis. That study revealed that even split-second judgments involve a complex, rapidly shifting mosaic of task-related evoked correlation patterns involving many electrodes over both hemispheres. Thus, simplistic views of neurocognitive processing may be the result of inadequate temporal resolution of rapidly changing neural activity.

The present study confirmed this by comparing move and no-move variants of the same spatial task. The results suggest that the tasks involve split-second changes in the relative localization and

lateralization of neural activity. A dramatic switching of the foci of patterns of evoked correlations is seen as the stimulus is anticipated, perceived, judged, and a response executed. These rapidly shifting patterns are consistent with network models of higher cognitive functions (Luria, 1977; Arbib and Caplan, 1979; Zurif 1980; Mesulam, 1981; and Gevins, 1981, 1983b). It should be understood that the simplicity of the patterns reported (Figure 6) is due to the fact that only the most significant results were diagrammed. The inclusion of results at lower significance levels would create more complex patterns, particularly in the RP interval. Further, in a separate within-task analysis, where each post-stimulus interval was compared with its prestimulus interval, it was evident that within-task differences were complex and increased in magnitude and anatomic distribution from interval to interval. This is consistent with a within-task interlatency analysis reported previously (Gevins, et al, 1981).

Individual Differences

Although the classification accuracies of the overall (multiperson) classification equations assessed on the data of the individual participants varied appreciably (Table 6), the existence of some invariant task-related patterns in 7 of the 9 persons was confirmed. The fact that the significant difference between tasks was also found at the P4 electrode set in the P3a interval when the data of one-person was subjected to NCP analysis also supports the inference of patterns which are invariant across people. Moreover, a nonparametric randomization test performed on the individual classification accuracies of the two groups of P's (#1-5 and #6-9) confirmed that the classification equations did not significantly differ between the two groups.

Is NCP Analysis Useful?

Analytic methodology is a critical factor in determining the precision and relevance of results in brain potential studies. NCP analysis uses modern signal processing and pattern recognition technologies to distinguish spatially and temporally overlapping task-related brain potential patterns. It builds on the vast body of ERP research by using the average ERP to determine person-specific time intervals during which successive stages of task-related processing may be assumed to occur. It then searches the single-trial, multichannel brain potential data with a mathematical pattern classification algorithm to extract spatial patterns which distinguish the two conditions of an experiment. As with other advanced approaches (reviewed in McGillem, et al, 1981 and Gevins 1980), it has the potential to reveal information not obtainable from averaged waveforms. Further studies will determine whether NCP analysis produces results meaningful enough to justify the large amount of computation required.

A full comparison of NCP analysis with linear multivariate methods is beyond the scope of this paper. Two linear tests were performed to give some indication of the differences between methods: post-hoc task x electrode-pair ANOVAs on selected variables, and the Bonferroni-corrected t-tests on the full set of single-trial correlations. The ANOVAs were limited to the 10 correlations of the most significant electrode sets determined NCP analysis: the P4 set in the P3a interval and the C3 set in the RP interval. Only the electrode-pair effect reached significance ($F(14,72) = 57.9$, $p<<.001$ and $F(14,72) = 48.6$, $p<<.001$, respectively). There was no significant task main effect or task x electrode-pair interaction. This result and the results of the t-tests (Table 4) suggest that the variable subset selection and the nonlinear, distribution-independent properties of the NCP Analysis were both important. This is consistent with two previous studies where this type of mathematical pattern recognition proved more effective than ANOVA and stepwise linear discriminant analysis (Gevins, et al, 1979a; Lieb, et al, 1981). Although the Bonferroni-corrected t-tests were significant for only two electrode pairs in one interval, at uncorrected significance levels ($p<.05$ or better), the significant electrode pairs did show a slight similarity to the NCP results. Of the significant Fz pairs in the prestimulus interval, 3 are identical to the prominent correlations determined by NCP Analysis (Fz-C3, Fz-C4 and Fz-T3), and the frontal distribution of significant pairs accords with the distinguishing Fz electrode set in the NCP results. For the N1-P2 and P3a intervals, however, only the T4-Pz electrode pair in the former interval and the P4-C4 pair in the latter correspond to prominent evoked correlations of the NCP analysis. In the RP interval the t-tests were focused on the frontal areas and included only two significant pairs from the NCP results (C3-Fz and C3-Pz).

In its present form, NCP Analysis seems able to extract patterns of task-related evoked differences from the obscuring effects of volume conduction and background EEG. Further research is being conducted using measures of interchannel timing and single channel power in paradigms involving manipulation of modality and responding hand. These studies may help elucidate the significance of inter-electrode evoked correlations accompanying neurocognitive processes.

ACKNOWLEDGEMENTS

H. Currens for manuscript preparation and artwork. H. Vaughan, D.O. Walter and C. Woods for critical reviews. E. Callaway of the Langley Porter Institute, D. Woodward of the Office of Naval Research, A. Fregly of the Air Force Office of Scientific Research, J. Miller of the Air Force School of Aerospace Medicine, and M. Brachman-Hoffman for research support.

BIBLIOGRAPHY

Arbib, M. and Caplan, D. Neurolinguistics must be computational. Behavioral and Brain Sciences, 1979, 2, 449-483.

Brazier, M. and Casby, J. Crosscorrelation and autocorrelation studies of electroencephalographic potentials. Electroencephalography & Clinical Neurophysiology, 1952, 4, 201-211.

Busk, J. and Galbraith, G. EEG correlates of visual-motor practice in man. Electroencephalography & Clinical Neurophysiology, 1975, 38, 415-425.

Callaway, E. and Harris, P. Coupling between cortical potentials from different areas. Science, 1974, 183, 873-875.

Desmedt, J. Active touch exploration of extrapersonal space. Proc. National Academy of Science, 1977, 74(9), 4037-4040.

Donchin, E., Kutas, M., and McCarthy, G. Electrocortical indices of hemispheric utilization. In S. Harnad et al. (Eds.), Lateralization in the Human Nervous System. New York, NY: Academic Press, 1977. Pp. 339-384.

Dumenko, V. Electroencephalographic investigation of cortical relationships in dogs during formation of a conditioned reflex stereotype. In Rusinov, V. (Ed.), Electrophysiology of the Central Nervous System, New York:Plenum Press, 1970.

Friedman, D., Vaughan, H. and Erlenmeyer-Kimling, L. Stimulus and response related components of the late positive complex in visual discrimination tasks. Electroencephalography & Clinical Neurophysiology, 1978, 45, 319-330.

Fuster, J. The Prefrontal Cortex. New York:Raven Press, 1980.

Gevins, A. and Yeager, C. EEG spectral analysis in real time. DECUS Proceeding, Maynard, Mass:Spring, 1972. Pp. 71-80.

Gevins, A., Yeager, C., Diamond, S., Spire, J., Zeitlin, G., and Gevins, G. Automated analysis of the electrical activity of the human brain (EEG): a progress report. IEEE Proceedings, 1975, 63(10), 1382-1399.

Gevins, A., Zeitlin, G., Yingling, C., Doyle, J., Dedon, M., Henderson, J., Schaffer, R., Roumasset, J. and Yeager, C. EEG patterns during cognitive tasks: I. Methodology and analysis of complex behaviors. Electroencephalography & Clinical. Neurophysiology, 1979(a), 47, 693-703.

Gevins, A., Zeitlin, G., Doyle, J., Schaffer, R. and Callaway, E. EEG
patterns during cognitive tasks, II. Analysis of controlled tasks. Electroencephalography & Clinical Neurophysiology, 1979(b), 47, 704-710.

Gevins, A., Zeitlin, G., Doyle, J., Schaffer, R., Yingling, C., Yeager, C. and Callaway E. EEG Correlates of higher cortical functions. Science, 1979(c), 203, 665-668.

Gevins, A. and Schaffer, R. Critical review of research on EEG correlates of higher cortical functions. CRC Reviews in Bioengineering, CRC Press, October 1980, Pp. 113-164.

Gevins, A., Doyle, J., Schaffer, R., Callaway, E. and Yeager, C. Lateralized cognitive processes and the electroencephalogram. Science, 1980, 207, 1005-1008.

Gevins, A. Pattern recognition of human brain electrical potentials. IEEE Transactions on Pattern Analysis and Machine Intelligence, 1980, PAMI-2(5), 383-404.

Gevins, A., Doyle, J., Cutillo, B., Schaffer, R., Tannehill, R., Ghannam, J., Gilcrease, V. & Yeager, C. New method reveals dynamic patterns of correlation of human brain electrical potentials during cognition. Science, 1981, 213, 918-922.

Gevins, A. Dynamic brain electrical patterns of cognition, in Third IEEE Conf. Eng. Med. Biol, New York:IEEE Press, 1981.

Gevins, A. Brain potentials and mental function: methodological requirements. In I. Alter (Ed.), The Limits of Functional Localization, New York:Raven Press, 1983a, In press.

Gevins, A. Brain potential evidence for lateralization of higher cognitive functions. In Cerebral Hemisphere Asymmetry: Method, Theory and Application, J. B. Hellige (Ed.), Praeger Press, 1983b. pp. 335-382.

Gevins, A., Schaffer, R., Doyle, J., Cutillo, B., Tannehill, R. and Bressler, S. Shadows of thought: Shifting lateralization of human brain electrical patterns during a brief visuomotor task. Science, 1983(a), 220, 97-99.

Gevins, A., Doyle, J., Zeitlin, G., Bressler, S. A trainable classification network algorithm for studying brain potential patterns of higher cognitive functions. IEEE Transactions on Pattern Analysis and Machine Intelligence, 1983(b), In Prep.

Lieb, J., Engel, J., Gevins, A., and Crandall, P. Surface and depth EEG correlates of epileptic foci and surgical outcome in temporal lobe epilepsy. Epilepsia, 1981, 22, 515-538.

Livanov, M. Spatial Organization of Cerebral Processes. New

York:Halsted (Wiley), 1977.

Luria, A. Higher Cortical Functions in Man. New York:Basic Books, 1977.

McGillem, C., Aunon, J. and Childers, D. Signal processing in evoked potential research. CRC Review in Bioengineering, 1981, 6(3), 225-265.

Mesulam, M. A cortical network for directed attention and unilateral neglect. Ann. Neurol. 1981, 10(4), 309-325.

Naatanen, R., Hukkanen, S. and Jarvilehto. Magnitude of stimulus deviance and brain potentials. In H. Kornhuber and L. Deeke, (Eds.) Motivation, Motor and Sensory Processes of the Brain: Electric Potentials, Behavior and Clinical Use. Amsterdam:Elsevier, 1980.

Renault, B., Ragot, R., Lesevre, N. and Remond, A. Onset and offset of brain events as indices of mental chronometry. Science, 1982, 215, 1413-1415.

Ritter, W., Vaughan, H. and Simson, R. On relating event-related potential components to stages of information processing. In Gaillard, A. and Ritter, W. (Eds.), Tutorials in Event-Related Brain Research, Amsterdam:Elsevier, 1983.

Simson, R., Vaughan, H., and Ritter, W. Scalp topography of potentials in auditory and visual go/no-go tasks. Electroencephalography & Clinical Neurophysiology, 1977, 43, 864-875.

Squires, K., Donchin, E., Herning, R., and McCarthy, G. On the influence of task relevance and stimulus probability on event-related potential components. Electroencephalography & Clinical Neurophysiology, 1977, 42, 1-14.

Teuber, H. The riddle of frontal lobe function in man. In M. Warren and K. Abert (Eds.), Frontal Granular Cortex and Behavior, New York:McGraw-Hill, 1964. Pp. 410-477.

Viglione, S. Applications of pattern recognition technology. In J. Mendel and k. Fu (Eds.), Adaptive Learning and Pattern Recognition Systems. New York:Academic Press, 1970. Pp. 115-161.

Walter, W. Slow potential changes in the human brain associated with expectancy, decision and intention. Electroencephalography & Clinical Neurophysiology (Suppl.), 1967, 26, 123-130.

Walter, W. and Shipton, H. A new toposcopic display system. Electroencephalography & Clinical Neurophysiology, 1951, 3, 281-292.

Zurif, E. Language mechanisms: A neuropsychological perspective. American Scientist, 1980, 68, 305-310.

LEGENDS

Figure 1 - Examples of stimuli for move and no-move trials. Arrow originated at center screen; its direction and the location of the target changed randomly across trials. The labels "Move" and "No-Move" did not appear in the actual stimuli.

Figure 2A - Electrode montage.

Figure 2B - 91 pairwise correlations were computed between the 15 electrodes.

Figure 2C - Anatomical constraints. The correlations of a principal electrode was measured with 10 other electrodes. The aOz electrode set is shown.

Figure 3 - The major peaks of the average event-related potential (ERP) and Neurocognitive Pattern (NCP) Analysis intervals determined from them. This illustration is an average of the data from the last four persons in the study; in practice, the peaks and analysis intervals were determined separately for each person.

Figure 4a - ERPs for Move trials (610 trials from P's #6-9).

Figure 4b - ERPs for No-Move trials (604 trials from P's #6-9).

Figure 5 - Subtraction ERP's (No-Move minus Move, 6 P's) showing the negative (N2) peak at 240 msec.

Figure 6 - Between-task NCP results obtained from single trial evoked correlations. The most significantly differing electrode set and its prominent correlations are shown in each interval.

Figure 7a - Average right parietal ERP of those Move trials correctly classified by the NCP analysis in both the P3a and RP intervals using correlation measures (195 trials from 4 people).

Figure 7b - Average ERP of correctly classified No-Move trials. P391 (P3a) and P530 (P3b) peaks are larger in the correctly classified No-Move trials (193 trials from 4 people).

Figure 7c - Average ERP of incorrectly classified, but behaviorally correct, Move trials (122 trials from 4 people).

Figure 7d - Average ERP of incorrectly classified, but behaviorally correct, No-Move trials. P3a is absent and P3b is smaller, thus resembling the correct Move ERP (121 trials from 4 people).

Table 1 - Number of trials, ERP peak latencies, centerpoints of the NCP single trial correlation analysis intervals, and average response

initiation latency (EMG onset) for each of the 9 participants.

Table 2 - Averaged P3a peak amplitude (in micro-volts) and correlated t-tests (df = 9).

Table 3 - Response Preparation (RP) interval: averaged slope of a straight line fitted to slow negative potential shift and correlated t-tests (df=9).

Table 4 - t-tests of correlations for the nine participants (1612 trials: 839 Move, 773 No-Move). Only those channel pairs showing a significant uncorrected t-value are listed. ($p<.05$ = 1.96, $p<.01$ = 2.57, $p<.001$ = 3.29. *Bonferroni-corrected t-value of 3.58 = $p<.05$.)

Table 5 - Simplified, single discriminant function classification equation. G(f) =1 for f>0, else G(f) =0; (X/Y) is the standardized, Fisher's z' transformed correlation value of the X-Y electrode pair. Individual trials whose classification function G(f) = 1 were assigned to the no-move class; those whose G(f) = 0 to the move class.

Table 6 - Classification accuracy for the P3a and RP intervals for each of the 9 participants using the equations derived from the whole group.

P	# Trials		ERP peaks (msec)			Analysis intervals centerpoint			EMG onset (msec)
	Move	No Move	N_1	P_2	No-Go P_{3a}	N_1-P_2	P_{3a}	RP	
1	42	33	164	236	452	218	452	587	971
2	36	36	164	236	388	200	388	523	913
3	39	30	176	243	482	228	482	617	791
4	42	39	164	236	462	210	462	597	1128
5	42	39	164	241	398	203	398	533	638
6	156	144	172	222	298	208	298	433	434
7	132	123	164	225	368	212	368	503	570
8	182	167	143	214	318	181	318	453	500
9	168	162	157	214	358	203	358	493	507
MEAN	(Total) 839	773	163	230	391	207	391	526	x=590 S.D. =190

Table 1

Average P3a Amplitude (μv)			Correlated $\underline{t}$	Uncorrected P<
	Move	No Move		
F_z	1.3	2.90	-2.95	.01
aCz	-.26	1.69	-2.91	.01
C_z	-.80	1.53	-3.16	.01
aPz	.14	2.30	-5.34*	5×10^{-4}
P_z	.49	2.32	-4.77*	.005
$_aO_z$	-.94	0.34	-2.28	.05
C_3	-.62	1.82	-3.82	.005
C_4	-.17	2.12	-4.44 *	.005
P_3	-.39	1.94	-2.97	.01
P_4	-.80	1.11	-3.05	.01

* Bonferroni $\underline{t}$ (15 comparisons, df = 7, $p<.05 = 4.35$

Table 2

	Average Slope RP Interval		Correlated t	Uncorrected P<
	Move	No Move		
Fz	.24	-.18	1.09	N.S.
aCz	.17	-.48	2.80	.05
Cz	.07	-.82	2.30	.05
aPz	.00	-.51	2.14	.05
Pz	-.03	-.69	2.10	.05
aOz	-.17	-.35	1.9	.05
C3	.24	-.50	3.5	.005
C4	.62	-.54	3.0	.01
P3	-.01	-.58	2.8	.05
P4	-.11	-.69	2.2	.05

* Bonferroni t (15 comparisons, df = 7) $p < .05 = 4.35$

Table 3

Correlation Electrode Pair	t Prestimulus Interval	t $N_1 - P_2$ Interval	t P_{3a} Interval	t RP Interval
$F_z - F_7$				2.24
$F_z - F_8$			2.88	
$F_z - T_3$	2.38			
$F_z - C_3$	3.12			2.42
$F_z - C_4$	2.60			2.08
$F_z - P_3$				2.16
F_z - pFz				2.58
F_z - aCz	2.38			
$F_z - C_z$	2.35			2.43
F_z - aPz				2.38
F_z -aOz				2.46
F8 -aCz	2.08		2.37	2.70
$F_8 - P_z$				3.13
$F_8 - P_3$				3.30
$F_8 - P_4$				3.16
$T_4 - P_z$		2.11		
$P_4 - C_4$		2.47	2.94	
aCz - C_3	2.60			
$T_4 - T_3$	2.29			
$C_4 - C_3$	2.17			
$F_7 - C_3$				3.20
$F_7 - T_3$				3.72*
F_8 - aFz			2.58	2.63
$F_8 - C_z$			2.50	3.34
F_8 - aPz				3.82*
F_8 -aOz				3.29
$F_8 - C_4$				3.56
aCz - C_z			2.09	
aPz - C_3				2.80
$P_z - C_3$				3.01
$P_3 - T_4$		2.22		
$P_4 - C_3$				2.51
T_4 - aPz		2.13		2.38
$T_4 - C_4$				2.70
T4 - P4				2.17

Table 4

*Bonferroni-corrected t; (100 comparisons, df = 120, $p < .05 = 3.58$)

Interval	Classification Equation
Prestimulus	G[-.089(Fz/T3)-.183(Fz/C4)+.355(Fz/P3)-.438/C3)
N1 — P2	G[.336(Pz/T3)-.471(Pz/F7)+.233(PzT4)-.130(Pz/aCz)
$P3_a$	G[-.323(P4/aOz)+.573(P4/C4)-.270(P4/aCz)
RP	G[-.697(C3/Pz)+.319(C3/Fz)+.480(C3/aOz)]

Table 5

Interval \ P	1	2	3	4	5	6	7	8	9	whole group
P_{3a}	64.4	55.0	53.2	51.7	55.1	52.5	58.7	51.5	54.4	55.1
RP	62.8	64.6	47.0	43.9	64.2	58.7	52.0	58.8	60.2	55.6

Table 6

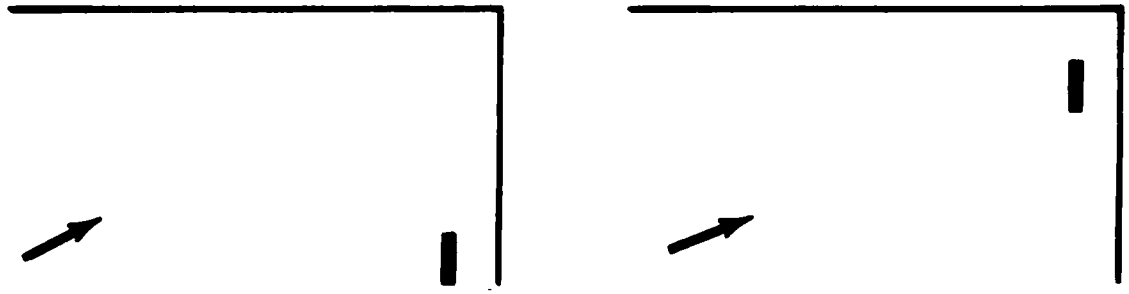

Fig. 1

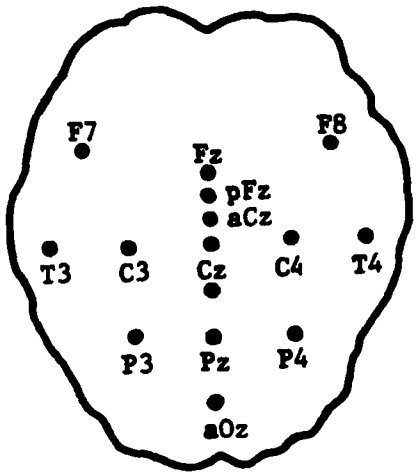

Fig. 2A

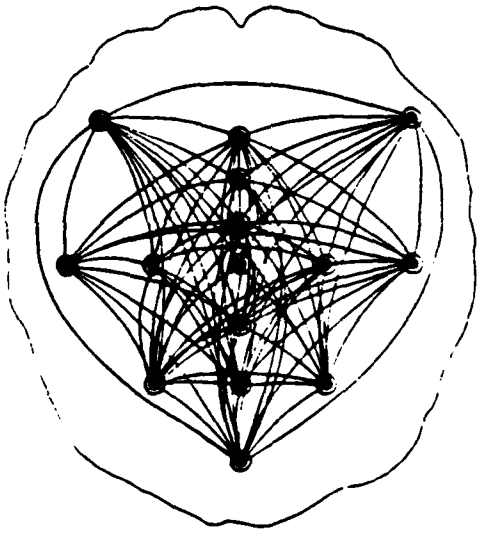

Fig. 2B

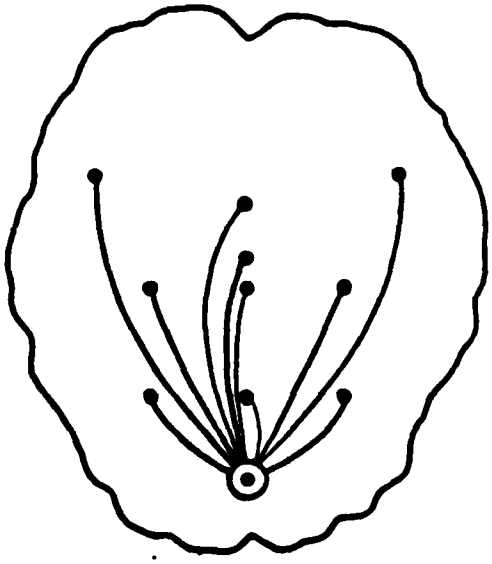

Fig. 2C

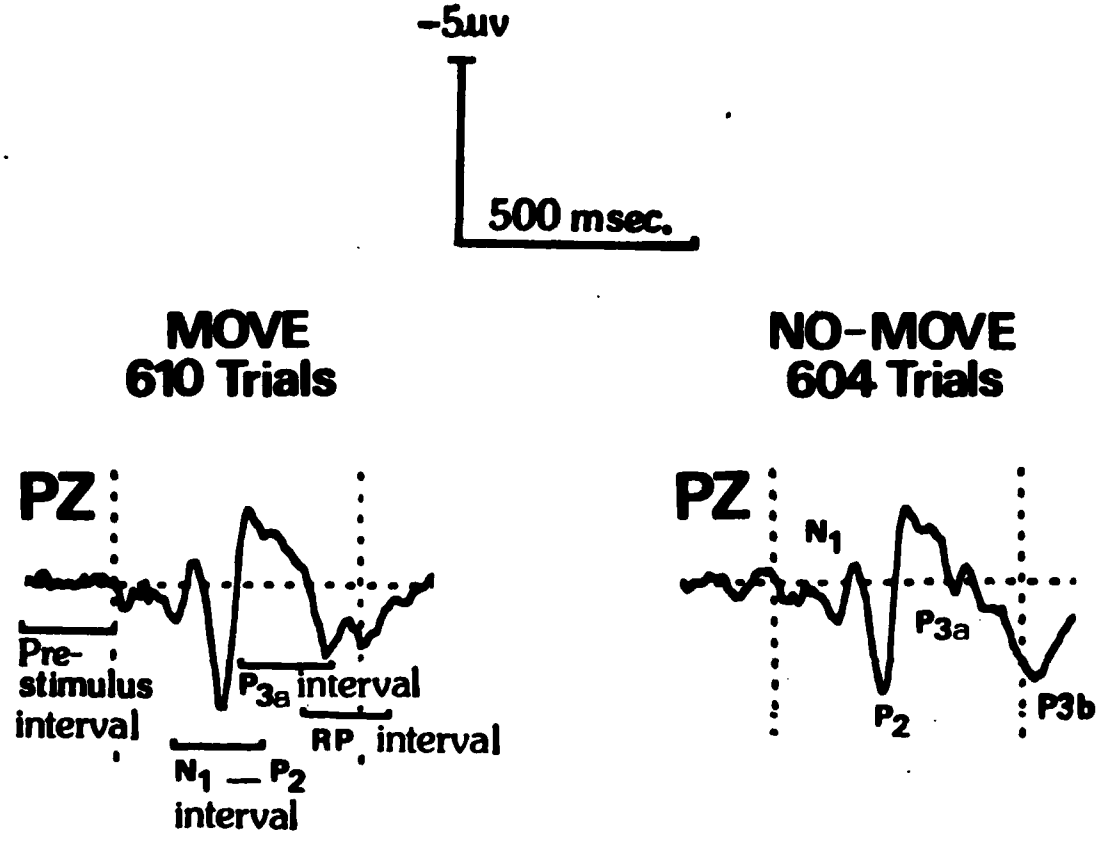
-5μv
500 msec.
MOVE
610 Trials
NO-MOVE
604 Trials
PZ
Pre-
stimulus
interval
P3a interval
RP interval
N1 — P2
interval
PZ
N1
P3a
P2
P3b

Fig. 3

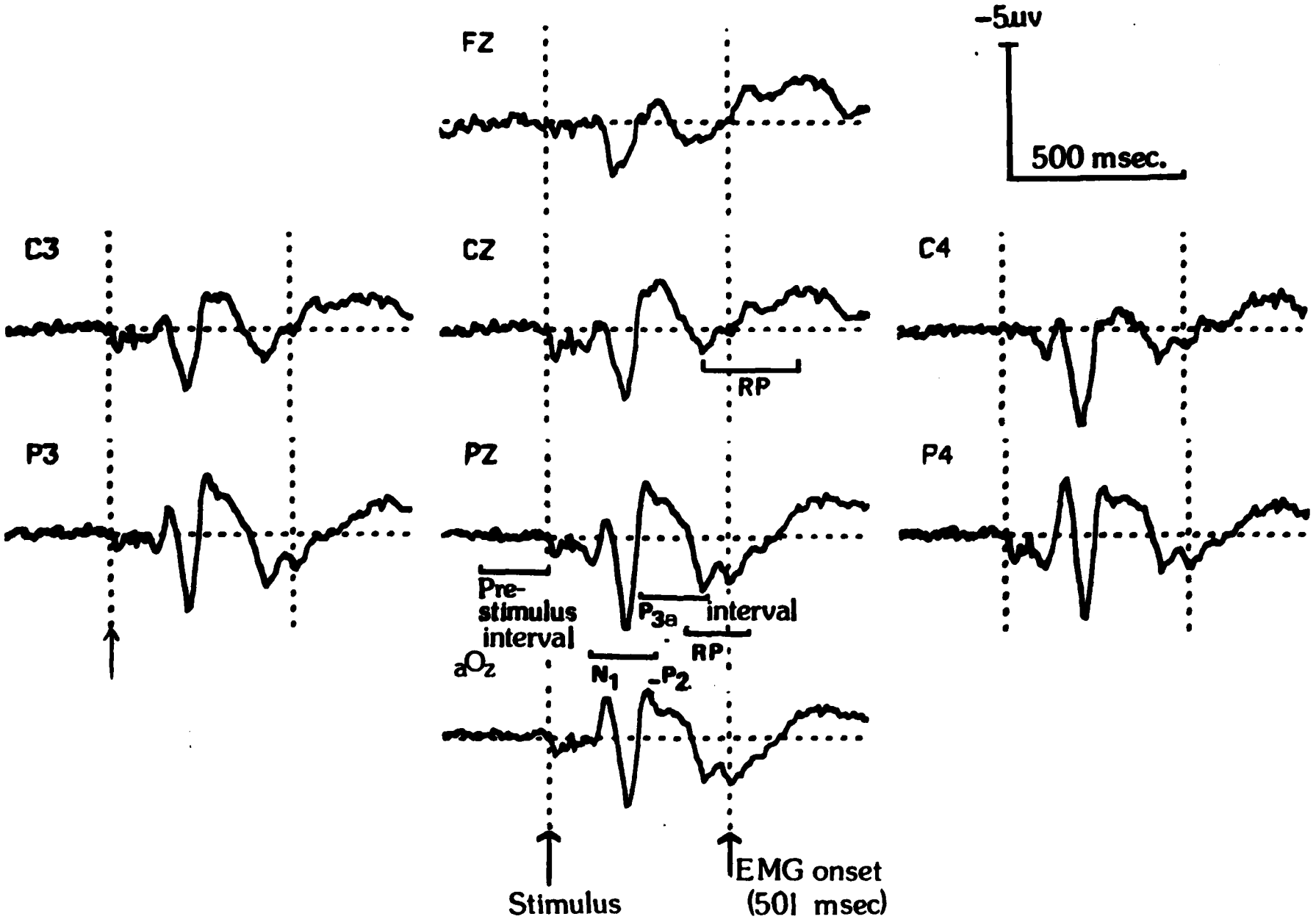
MOVE
(610 Trials)
FZ
-5μv
500 msec.
C3
CZ
C4
RP
P3
PZ
P4
Pre-
stimulus
interval
P3a
interval
RP
aO2
N1
P2
Stimulus
EMG onset
(501 msec)

Figure 4a

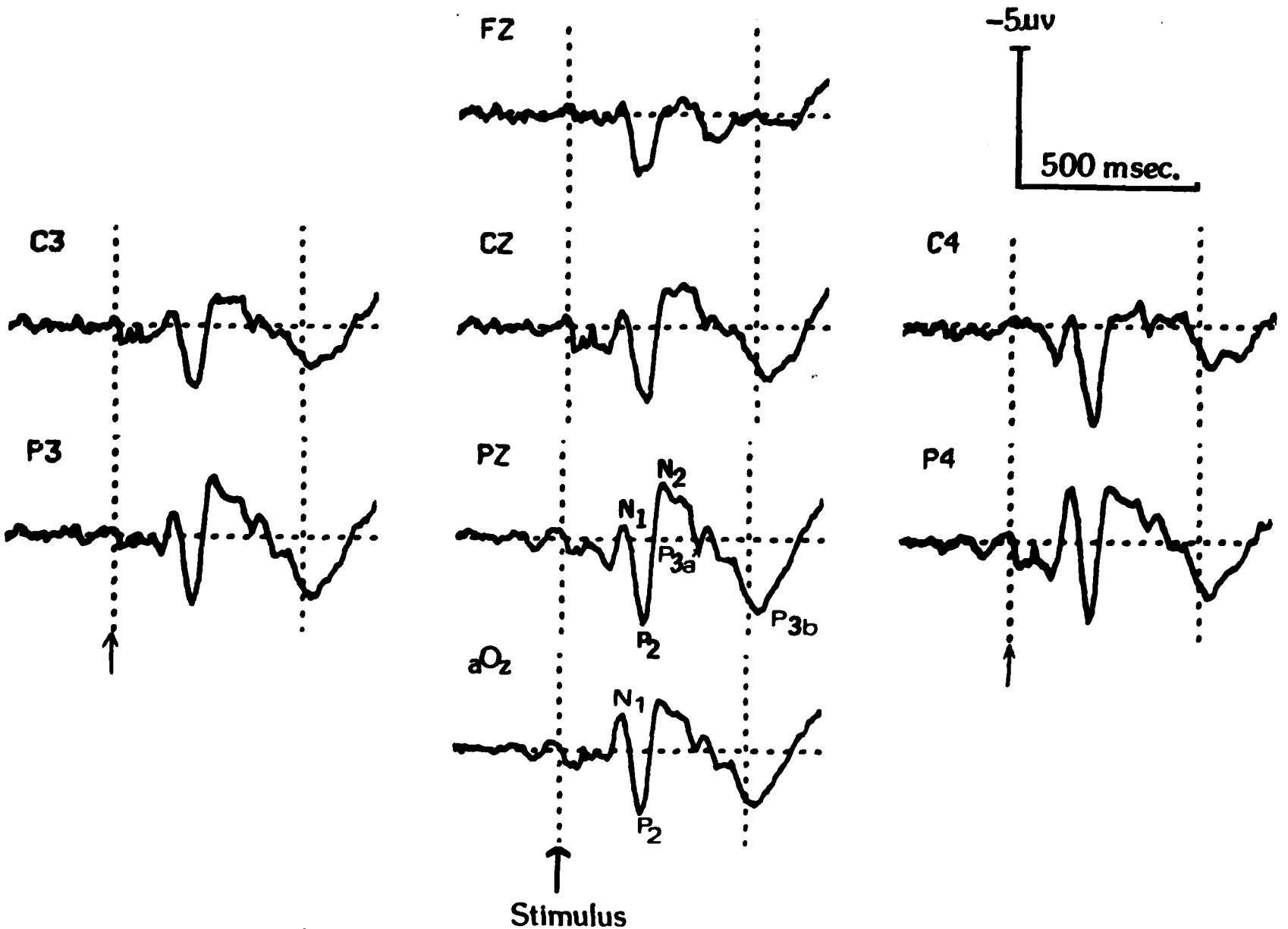
NO-MOVE
(604 Trials)
FZ
-5μv
500 msec.
C3
CZ
C4
P3
PZ
P4
N2
N1
P3a
P3b
P2
aO2
N1
P2
Stimulus

Figure 48

NO-MOVE Minus MOVE

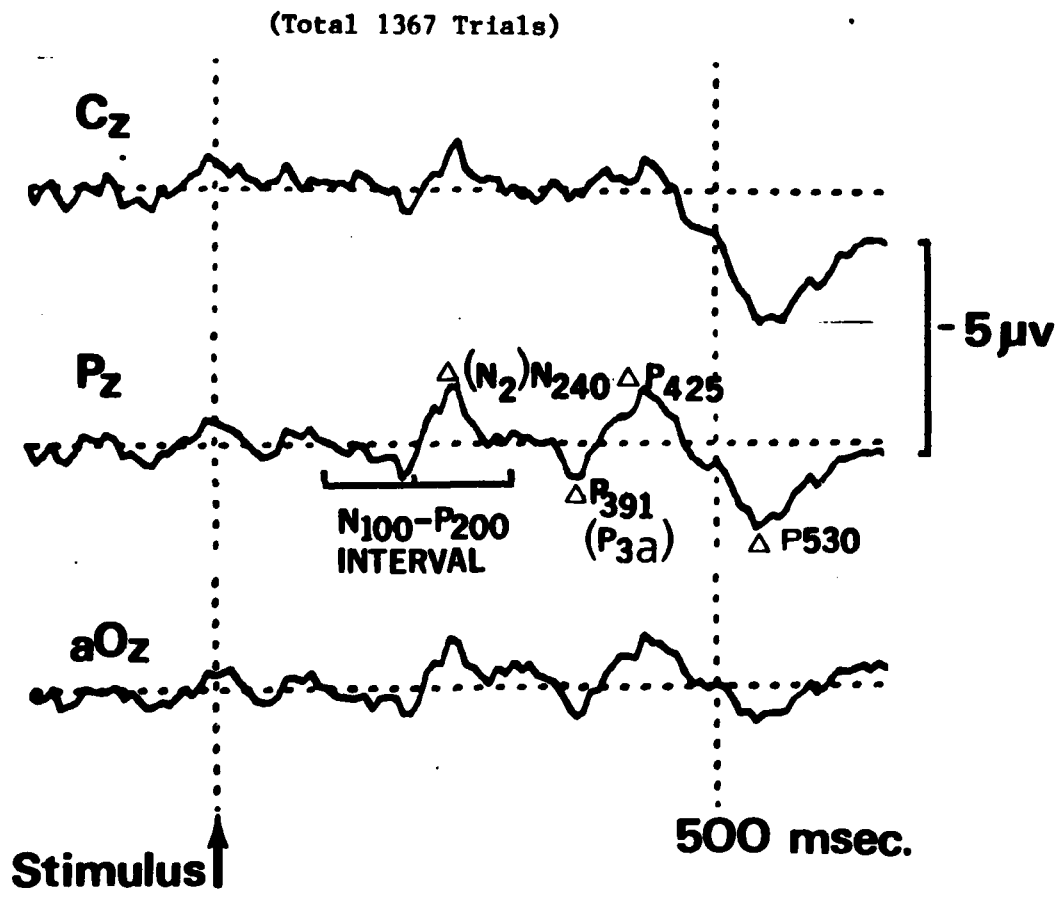

Figure 5

MOVE vs. NO-MOVE
(NCP Analysis)

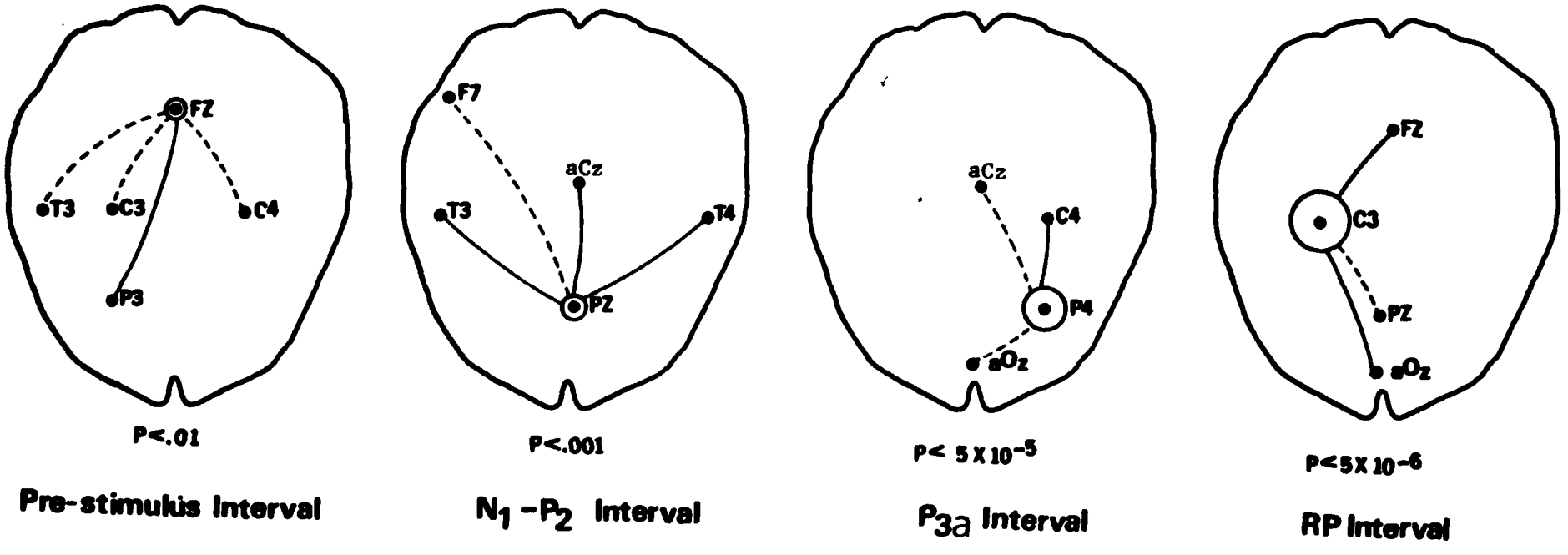

Figure 6

V. Distinct Brain-potential Patterns Accompanying Behaviorally Identical Trials (Also sponsored by the Air Force Office Scientific Research)

In order to examine patterns used by the pattern recognition algorithm to define the move and no-move trials, the classification assigned by the algorithm to each trial of the testing data was noted. In all cases, the data were behaviorally correct. Trials for which classification was correct for both P3a and RP intervals were called correct; those with incorrect classification for both intervals were called incorrect. This was done for both move and no-move conditions, resulting in four classes: (a) correct move, (b) correct no-move, (c) incorrect no-move, and (d) incorrect move. Unfiltered ERPs were formed for each class for the data of the last 4 people in the study (Figure 1).

The main difference between correctly classified move and no-move ERPs was the positive P3a and P3b peaks at approximately 365 and 530 msec post-stimulus, respectively. Comparing Figure 1c with Figure 1b, the incorrect no-move ERP is seen to lack a P3a peak and have a smaller P3b peak, thus resembling the correct move ERP. The incorrectly classified move trials (Figure 1d) have a more distinct P3b peak than the correctly classified move trials (Figure 1a), thus resembling the correctly classified no-move ERP.

Another obvious difference between correctly and incorrectly classified ERP's, both move and no-move, was the strong pre-stimulus alpha 'train' in incorrectly classified ERPs. This dissimilarity is clearly seen in alpha band-pass filtered averages (Figure 2). In both the correct and incorrect move conditions there are alpha band ERPs which occur at the same post-stimulus time (in phase). In the incorrectly classified waveform the pre-stimulus alpha is much larger than in the correct, and is phase reversed. The incorrect ERP appears to undergo a phase adjustment prior to the zero-crossing at approximately 90 msec post-stimulus, which occurs at the same time in the correctly classified trials, and is followed by a negative peak at 160 msec in both. This peak corresponds to the N163 peak in the unfiltered ERP. This could reflect a timing process which regulates the activity of sensory cortex in preparation for incoming stimuli (the old idea of the 'neuronic shutter'). These alpha-band filtered ERP's are also clearly different in the P3a and RP intervals where the classification was made. The high prestimulus alpha in the incorrectly classified trials may be related to cognitive state, so that incorrectly classified trials are qualitatively different, perhaps due to automatic processing. Alternatively, incorrectly classified trials may be those with a particular alpha phase at stimulus onset, resulting in enhanced summation of pre-stimulus waves, and difference in post stimulus activity. These possibilities are being further investigated since the results show that different neural patterns may accompany the same behavior.

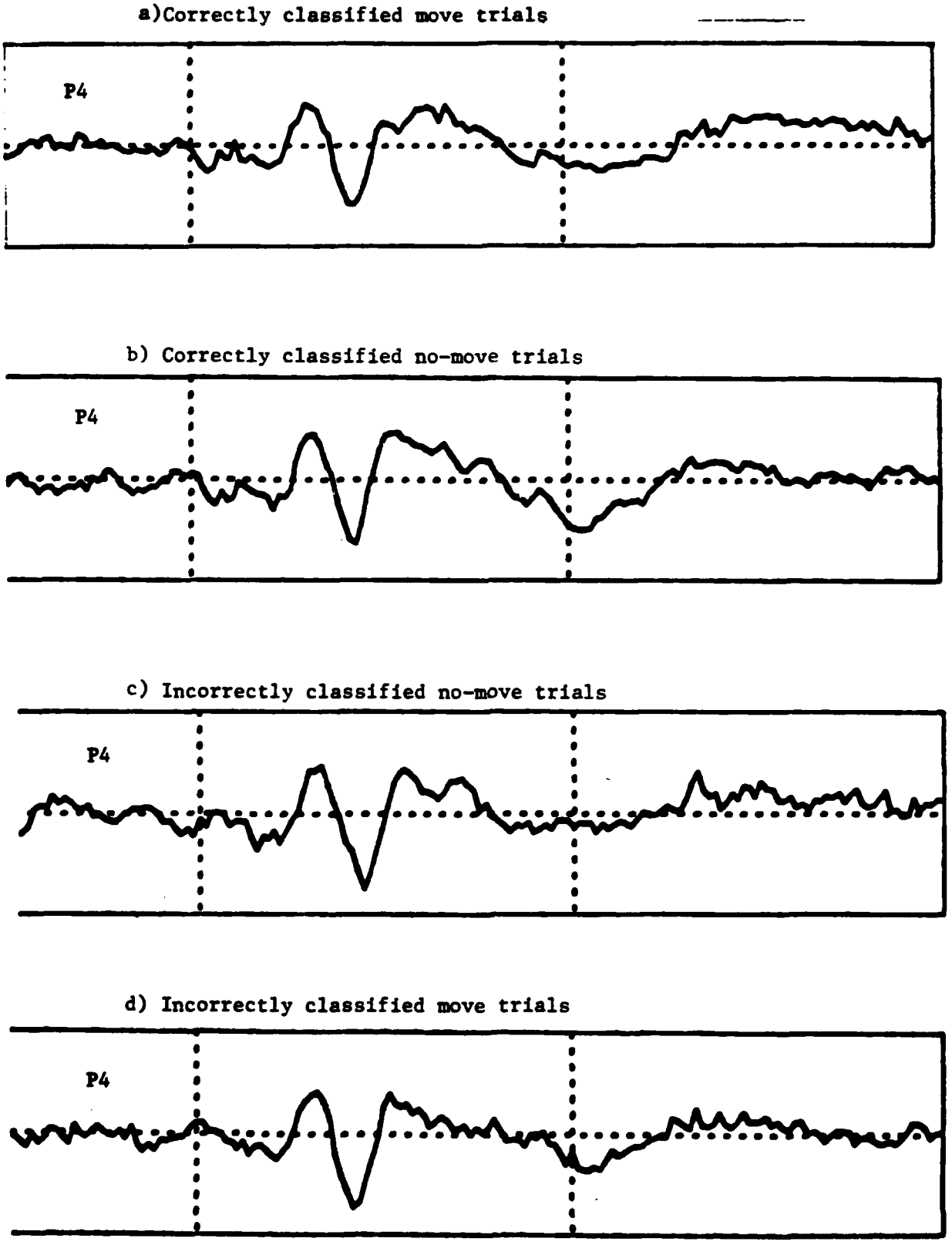

Figure 1 - Average ERPs for trials which were correctly and incorrectly classified by the NCP analysis.

CORRECTLY CLASSIFIED MOVE TASK

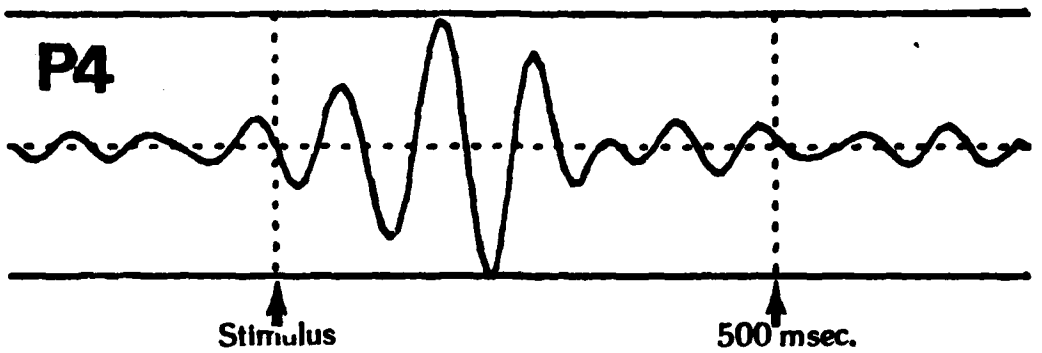

INCORRECTLY CLASSIFIED MOVE TASK

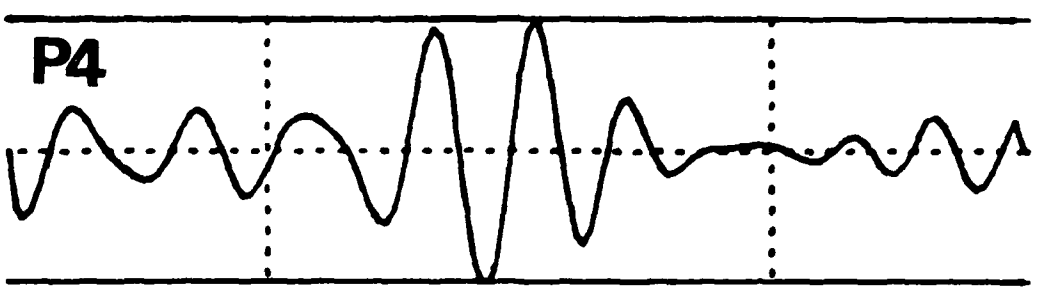

(317 Trials Total, 8-15 Hz)

Figure 2

VI. Computer Systems Development

During the current period, computing facilities have been expanded by the acquisition of used Digital PDP-11/60 and PDP-11/45 computer systems. The 11/60 is equipped with an Able memory expansion unit and 1.25 Mb memory, a 160 MB Winchester disk drive, a 75 ips tape drive, two 5 MB cartridge disks and a 16 line terminal multiplexor. The 11/45 has 256 KB memory, a 1.5 MB and two 2.5 MB cartridge disks, an 8-line terminal multiplexor and an LPA-11 DMA interface with associated modules for 64 channel laboratory data collection and D/A operations. Both systems run the RSX11-M V.4.0 operating system. SYSGENS are performed in the laboratory. Multiuser word processing is supported using the Word 11 system. There are two 1200 baud remote lines.

We have nearly completed reprogramming and testing the major components of the signal processing subsystems of the ADIEEG system (see Fig. 1). Functions of the components have been expanded and a major new program has been implemented for automated trial selection. A program has been written to transfer 7-track PDP15 data tapes to the 9-track PDP11 format. This data translation program, DATCOP, computes a common average reference. DATCOP is designed to maintain compatibility between our current data base and experimental data which will be collected with our new system. The aim is to replace as much of the manual recording of information as possible by the incorporation in future data-bases of automatic documentation of collection activites, special situations (e.g. bad channels), setup details, and cross-referenced files.

The averaged evoked-potential package, ADIERP (consisting of ADIPIX, ADIGRAF, and ADIPLT), has been completely rewritten. Both ADIPIX, the program which performs averages, and ADIGRAF, the program which produces graphs, take advantage of available virtual memory for speed rather than using disk files for data accumulation. Capacity is up to 55 channels for up to 4 files for data accumulation, and up to 55 channels for up to 4 events. Events are selectable for each task type and bad channels are eliminated for each trial. The system is flexibly data-driven with regard to numbers of channels and points per record. The graphing is done on events and channels chosen by the user; up to 15 files may be averaged or different averages may be subtracted; a compatible output file may be created. Graphing may be done immediately or, if the user prefers, written to a plot file for later graphing by ADIPLT. A faster version of the program is under development.

ADIDOT has been converted to the PDP11/60. This program reads the raw data files and produces comprehensive observation files of behavioral variables describing each trial, as well as arousal and eye movement measures derived from the electrophysiological data.

ADIFX is a feature extraction program which operates on single-trial EEG data and computes specified measurements (e.g. single-channel power or correlations between channels) which are output to be used as features for pattern recognition. The program has been extensively

revised and modified to utilize the capabilities of the PDP 11/60 computer. It has been improved to operate on different events within an experimental trial. It has been expanded for production of up to 1000 features for each trial. It now allows interactive dialog for specificiation of up to 55 EEG channels, 15 time windows, 15 frequency filters and 400 trials. The current version produces measurements of power. Measures of zero-lag cross-correlation, maximum lagged covariance and lag number are under development. A faster filter function is being implemented.

ADIMRG, the data selection and merging program, now allows selection of observations either by serial number in the input file or by original period number in the raw data file. This allows selection by the automatic reading of standard period files maintained for each raw data file. A separate program, ADINRM, now performs the data normalization for all variables within each participant for up to 12 participants simultaneously, using virtual memory rather than disk files to accumulate data.

ADISORT is a menu driven program to interactively select trials from feature files. The main process, called a "sort", involves selecting trials by adjusting the limits on specified variables. Creating a sort involves specifiying a feature file, a set of variables, and an observation range (or period list) for that file to be included or deleted from the sort. The program has the capacity for dealing with two sorts. Menu commands include: interactive trial selection, t-tests between the two data sorts for all variables, creation of output report files, and creation of graphics output.

ADISAM, the pattern recognition program, has been completely parametrized for ease in configuring it to particular applications (eg. maxima of the number of passes, candidate units per pass, number of units selected per pass, connections per candidate, variables per observation, observations per input file, variables per design, designs per run. It has improved dialog for easier use, systematic rather than random unit generation with elimination of duplicates, option to suppress reweighting (initializing each pass) for certain kinds of studies, improved handling of unequal numbers of samples in the two classes, optional output of pattern weights and pattern losses to enable studies of classification performance. A small version of it will run on the 11-45 and a larger faster version on the 11-60.

ADIEEG SYSTEM FOR NEUROCOGNITIVE PATTERN RECOGNITION

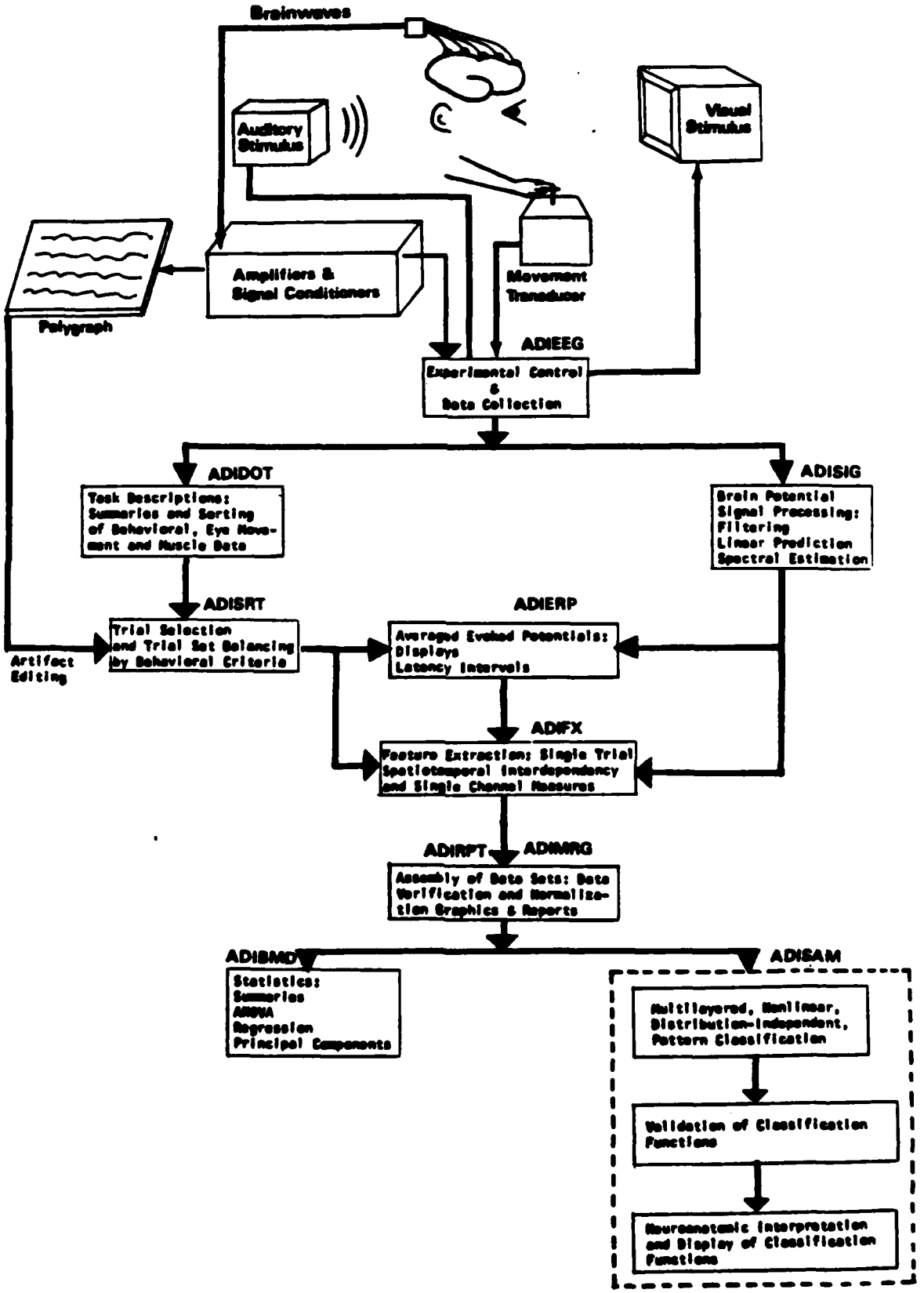

VII - Elimination of Extra-cerebral Electrical Contaminants in Single-trial Data

A. Pilot Study for Muscle-Potential (EMG) Filter

The frontalis and temporalis muscles of the scalp lie directly beneath potentially important recording sites of the lateral frontal and temporal areas. Their electrical activity contaminates brain potentials at these locations and at more distant sites. Simple low-pass filtering is inadequate for removing these contaminants for two reasons: low-frequency components are present in the EMG potentials, and we wish to analyze brain signals up to 100 Hz. As is the case with eye-movements, contractions of these muscles could vary systematically between tasks or with increasing taskload. A pilot study was conducted to investigate the requirements for constructing a digital filter to separate scalp muscle potentials from those generated by the brain.

We found that closely-spaced pairs of bipolar electrodes (about 0.75 cm apart) are preferentially sensitive to near-field activity, and thus pick up the activity of muscle motor units with little contribution from brain potentials. These bipolar electrode pairs might be used as detectors of muscle activity and as sources of data for the design of a digital EMG filter by allowing measurement of the morphology and topography of muscle potentials.

The results of several test recordings may be summarized: 1) temporalis and frontalis muscles are quite active, especially during cognitive task performance; 2) there is great variability between persons as to amount of baseline muscle activity and ability to "quiet" scalp musculature with biofeedback; 3) when asked to voluntarily contract temporalis musculature and then relax, individual small motor units can remain active for a long period of time; 4) unequivocal muscle spike activity seen with the closely-spaced bipolar electrodes appears similar in form to fast brain-potential activity seen in ordinary "common-referenced" scalp recordings; 5) the muscle potential field is quite large with standard-spaced, common-referenced electrodes, but is usually small with the closely-spaced bipolar electrodes; and 6) a number of closely-spaced bipolar electrodes (4-16) are required to adequately sample the activity of scalp muscles.

In another series of recordings fine (26-gauge) EEG needle electrodes were employed. When placed in the temporalis and frontalis muscles at spacings of less than 1 cm they are almost entirely sensitive to near-field EMG activity. Bipolar needle electrodes may be used to record EMG signals while a mixture of EEG and EMG is simultaneously recorded by "common referenced" cup electrodes at the same locations. These dual recordings could form the data-base for the design of a digital filter for removal of EMG contamination in normal recordings (ie. without direct measurement of EMG signals by needle electrodes).

Implementation of an EMG filter has been postponed due to the

requirement of a sampling rate of 1024 samples/second to adequately characterize muscle spike morphology, a rate beyond the current capability of our system.

B. Proposed Method for the Removal of Eye-movement Artifacts from Single-trial Data

1. Introduction.

A number of methods have been used in the attempt to remove the contamination caused by eye-movements from scalp-recorded brain potentials (Hillyard and Galambos, 1970; Girton and Kamiya, 1973; Verlager, et al, 1982; Fortgens and De Bruin, 1983; Gratton, et al, 1983). Of these methods, only that of Gratton, et al, takes into account the different topographies of the electrical potentials due to eye-movements and blinks (Overton and Shagass, 1969). These methods were of varying effectiveness, and most importantly from our point of view, they are aimed at removing cumulative effects of eye-movement artifacts from ensembles of trials, not from data to be analyzed as single trials. The methods are based on the probability distribution of the EEG and eye-movement potentials using the first moment of these distributions - the averages. It seems likely that a better estimate of the correction factors could be obtained by using at least the second moments of the observations. This section outlines a proposed method for using second order information to obtain a better estimate of the correction factors involved by minimizing the cross-correlation between the recorded eye movements and the corrected EEG on a single-trial basis by the technique of instrumental variables.

The potentials generated by eye-movements and blinks (electro-oculogram, or EOG) is traditionally measured from pairs of electrodes placed on the skin at the outer canthi, and above and below the orbit of one eye. These record the potentials due to horizontal (saccadic) and vertical (primarilly blink) movements, respectively. The source of the potentials measured in the EOG is primarily the CorneoFundal Potential (CFP). This is a dc potential between the cornea and the fundus (back) of the eye. This causes the eye to act as an electrical dipole. In the case of vertical or horizontal eye movements, it is the rotation of this dipole which produces the measured potential changes. In the case of eyeblinks, the eyelids alter the contours of the potential field of the CFP by acting as sliding resistors (Oster & Stern, 1980). For example, extension of the lid increases the conductance between the dipole and the recording electrodes. This indicates that a different model for propogation of blinks and eye rotations should be used.

2. The Model. The objective is to obtain an optimal estimate of electrical activity originating from the brain at a given scalp electrode (which contains both brain and eye-movement potentials) by using a concurrent recording of EOG potentials from electrodes placed near the eye. This is depicted schematically in Figure 1. In order to simplify the problem at the outset, the assumption is made initially that the system is linear, and so the model of Figure 2a is obtained. Here, the three observed signals are the horizontal EOG (HEOG), the vertical EOG (VEOG), and the EOG-contaminated EEG, denoted

x_h, x_v, and H respectively. The system is modeled as ratios of linear operators Ax's and Bx's. The underlying EEG activity is denoted as R, and the contribution to the measured EEG signal from the EOG's is denoted Y.

In order to simplify the mathematical derivations, the system is recast in an equivalent form in Figure 2b. To see that this system is equivalent, note that B is now the product of $B_h x$ and $B_v x$, and that the A's now have additional roots to accomodate the 'extra' roots introduced into each branch by the new B.

The method is to be implemented on a digital computer, so it is reasonable to represent the system in state-space form. In this way, a vector U can be defined as

$$U^T = [u(t=0)\ u(t=-1)\ u(t=-2)\ \ldots\ u(t=-n)] \qquad (1)$$

where u(t) denotes the signal u at time t, and n corresponds to the estimated order of the system. Similarly, an operator can be defined as a vector of polynomial coefficients as in

$$D = [d_1\ \ d_2\ \ d_3\ \ \ldots d_n\ ] \qquad (2)$$

In this way, the operator D operating on the signal U is represented as

$$U^T D. \qquad (3)$$

Now an augmented signal vector is defined

$$X^T = [X_H^T \mid X_V^T] \qquad (4)$$

and a similar augmented coefficient vector is defined

$$A^T = [A_H^T \mid A_V^T].$$

The system now can be represented as in Figure 2c. (Note that more accurate representation is that of Figure 2 d. The other diagrams given are merely shorthand for this. The state variable generator depicted here is a memory element, providing values for x(t=-1), x(t=-2), etc.) Figure 2c is equivalent to Figure 2a, but is simply recast to simplify the mathematical manipulation.

3. The Method of Instrumental Variables

It is presumed that an optimal estimate of the coefficients of the system depicted in Figure 2 can be obtained by minimizing the cross-correlation between the recorded eye movements and the estimated clean EEG. A method for operations of this type has been developed, and is called the method of instrumental variables.

The method assumes an *a priori* estimate of the coefficients,

applied in a recursive manner, until no significant change is made in the estimate of the coefficients.

In the following, $\tilde{D}$ will denote a noise-free estimate of the quantity D, and $\hat{D}$ will denote the measured quantity D (presumably contaminated, or noisy).

Now referring to the system in Figure 2,

$$X^T A B^{-1} = Y^T \tag{6}$$

or

$$X^T A - Y^T B = 0. \tag{7}$$

At this point, it is remarked that choice of one coefficient in either A or B is arbitrary. For this derivation, the coefficient b_1 will be chosen as

$$b_1 = 1. \tag{8}$$

Now equation (7) can be written as

$$X^T A - Y_A^T B_A = y(t=0) = y_1 \tag{9}$$

where

$$\begin{aligned} Y_A &= [\, y(t=-1) \;\; y(t=-2) \;\; \ldots \;\; y(t=-n) \,] \\ &= [\, y_2 \;\; y_3 \;\; \ldots \;\; y_{n+1} \,] \end{aligned} \tag{10}$$

and

$$B_A^T = [\, b_2 \;\; b_3 \;\; \ldots \;\; b_{n+1} \,]. \tag{11}$$

Now a signal vector is defined as

$$S^T = [X^T \mid -Y_A^T \mid 1\,] \tag{12}$$

and a coefficient vector

$$C = [\, A \mid B_A \mid c_{2n} \,]. \tag{13}$$

and (9) becomes

$$S^T C = y. \tag{14}$$

If measurements are taken repeatedly now, the signal vector S is transformed into a signal matrix [S] given by

$$[S]^T = \begin{bmatrix} x_1 & x_2 & \cdots & x_n - y_1 & \cdots & -y_m & 1 \\ x_2 & x_3 & \cdots & x_{n+1} - y_2 & \cdots & -y_{m+1} & 1 \\ & \vdots & & \vdots & & \vdots & \\ x_k & x_{k+1} & \cdots & x_{n+k-1} - y_{k-1} & \cdots & -y_{k+m} & 1 \end{bmatrix} \qquad (15)$$

Now (14) becomes

$$[S]_k^T C = Y_k^T \qquad (16)$$

Observing that the signal y is unavailable for measurement, the measured signal w is substituted into the equation for y in all places. Since w is noisy, the equation (16) is no longer an equality. Denote the difference as e, and (16) becomes

$$[\hat{S}]^T C - W^T = E^T \qquad (17)$$

where $[\hat{S}]$ is now composed of the measured x's and the noisy outputs w.

Now referring to Figure 3, and letting $\tilde{A}$ and $\tilde{B}$ denote estimates for A and B, observe that a noise free estimate of Y can be obtained by

$$\tilde{Y}^T = X^T \tilde{A} \tilde{B}^{-1}. \qquad (18)$$

Now note that the estimate for the EEG ($\tilde{R}$) is given by

$$\tilde{R} = W - \tilde{Y} \qquad (\tilde{R} = E) \qquad (19)$$

Letting $\tilde{Y}$ replace Y in the signal matrix [S], we obtain the noise free estimate of the signal matrix, $[\tilde{S}]$, where

$$\tilde{S}^T = [\, X^T \,|\, \tilde{Y}_k^T \,|\, 1 \,]. \qquad (20)$$

Letting $\tilde{C}$ represent the inital estimate for C, and ΔC the correction to minimize the correlation between $\tilde{R}$ and X,

$$C = \tilde{C} + \Delta C\ , \qquad (21)$$

where

$$\Delta C = (\tilde{S}\hat{S}^T)^{-1} \tilde{S}(W^T - \tilde{S}\tilde{C}) \qquad (22)$$

provides the optimal estimate for C. This method is applied recursively, letting $\tilde{C}_i = \tilde{C}_i + \Delta C$.

This method relies on a fairly good initial estimate of the coefficient vector in order to converge. One way to obtain this is to use a least squared error algorithm. For this,

$$\Delta C = (\hat{S}\hat{S}^T)^{-1} \hat{S}(W^T - \hat{S}^T \tilde{C}). \qquad (23)$$

This method attempts to minimize the residual, R, which in this case is not what is desired at all, since R corresponds to the EEG signal estimate. Also, the least squared error algorithm diverges upon repeated application. (See appendix also)

4. Analysis of method

The method which will be used to evaluate these results is summarized below:

Deviation from 'true' ERP:

It will be assumed that the best estimate of the ERP is obtained through the traditional method of rejecting trials in the average which had eye activity above a low baseline. If the ERP computed with inclusion of corrected trials is more similar to this true ERP than the ERP computed with inclusion of all trials (but uncorrected), then the method is valuable.

Reduction in variance:

Since some of the variance in response between trials is due to eye movement, it is expected that removal of eye movement potentials from the EEG would remove some source of variance between trials. Therefore, if the variance between trials is decreased, the method can be assumed to have some success.

5. Problems with the method and points of extension

One problem with the method is that a good guess for the order of the system is needed prior to beginning computation. Underestimation of the order leads to exceptionally poor results, and overestimation leads to inclusion of roots that do not exist. The former is evident merely from observation of estimates that do not nearly fit the observations. The latter is evident when the estimation places poles very close to zeros, and thus produces poles with very little residue. When underestimation is suspected, merely reapplying the technique with higher order estimation is enough to improve the result. In the case of overestimation, residues are calculated for each pole, and those falling below a certain threshold are rejected.

The assumption of a linear system may be incorrect. This is a fundamental assumption allowing this technique to work, however there are methods by which non-linearities of a certain class may be modelled and estimated. Typical block diagrams for this type of system are shown in Figure 4..

There is some contamination of the EOG by EEG. This prevents the signals X in the model from being completely observed. In this case, one of two possibilities for correction may be used. The first, and initially preferable, is to obtain some measure of eye movement that is truly uncontaminated by the EEG. Methods exist which detect motion of the eyeball using light reflected off the cornea. Since this

method does not rely on electrical potentials measured from the skin, it should provide a direct measure of EOG without contamination by EEG. The second method is to use information regarding the spectral distribution of the EEG and EOG, and apply some form of whitening filter to the EOG before using the information in the signal matrix. This method probably will not prove to be useful, since the spectra of the EEG and EOG are very similar.

The volume of data is immense. A typical experiment might collect 400,000 or more measurements per EEG channel, and so in its most basic form, one dimension of the signal matrix should be 400,000. Clearly, some method of data reduction must be employed here. Since the system can be assumed to be fairly stable over an intermediate period of time, an estimate of the system can be made, and then that estimate used to simply process the EOG data and subtract it from the EEG measured. If this is done, it would seem to be wise to periodically update the estimate, or at least verify that it is still approximately correct.

6. Bibliography

Fortgens, C., and DeBruin, M.P. Removal of eye movement and ECG artifacts from the non-cephalic reference EEG. Electroenceph. Clin. Neurophysiol., 1983, 56:90-6.

Girton, D.G., and Kamiya, J. Simple on-line technique for removing eye movement artifacts from EEG. Electroenceph. Clin. Neurophysiol., 1973, 34:212-16.

Gratton, G., Coles, M. and Donchin, E. A new method for off line removal of ocular artifact. Electroenceph Clin. Neurophysiol., 1983.

Hillyard, S.A. and Galambos, R. Eye movement artifact in the CNV. Electroenceph. Clin. Neurophysiol., 1970, 28:173-82.

Oster, P. and Stern, J. Electoroculography. In Martin and Vennables (eds.), Techniques in Psychophysiology, Wiley and Sons, 1980.

Overton, D.A. and Shagass, C. Distribution of eye movement and eyeblink potentials over the scalp. Electroenceph. Clin. Neurophysiol., 1969, 27:544-49.

Verlager, R., Gasser, T. and Mocks, J. Correction of EOG artifacts in event-related potentials of the EEG: Aspects of reliability and validity. Psychophysiology, 1982, 19:472-80.

Figure 1

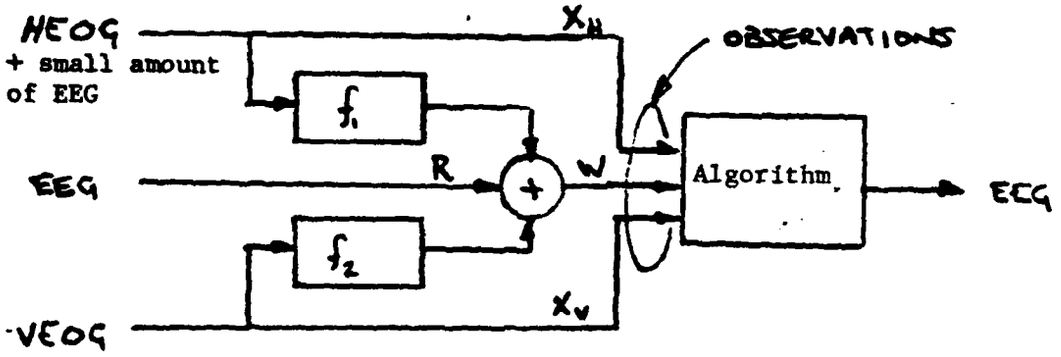

Figure 2

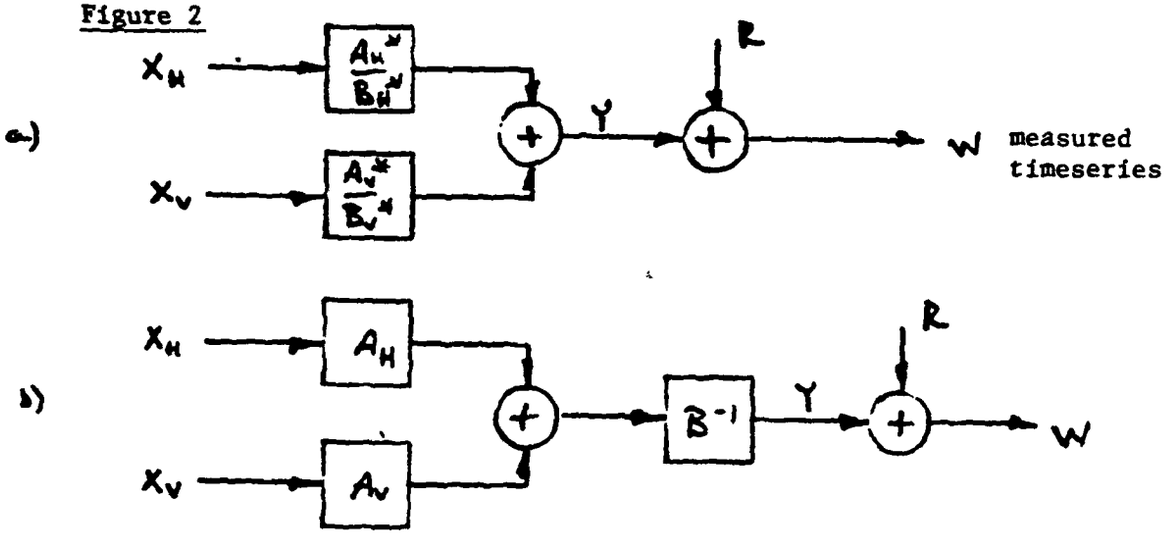

$$A_H B^{-1} = A_H^* B_H^{*-1} \quad ; \quad B^{-1} = B_V^{*-1} B_H^{*-1}$$
$$A_V B^{-1} = A_V^* B_V^{*-1}$$

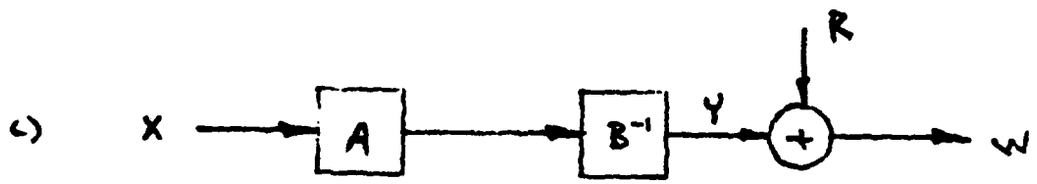

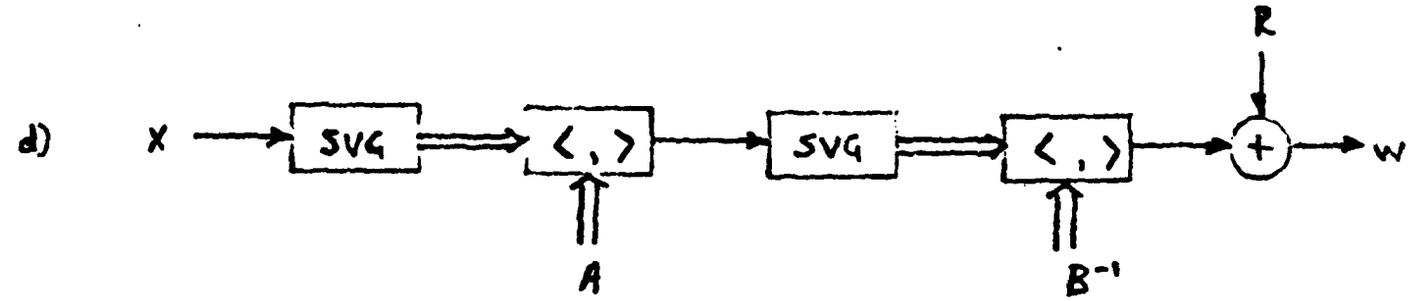

SVG - STATE VARIABLE GENERATOR. ⟨ , ⟩ - DOT PRODUCT

Figure 3

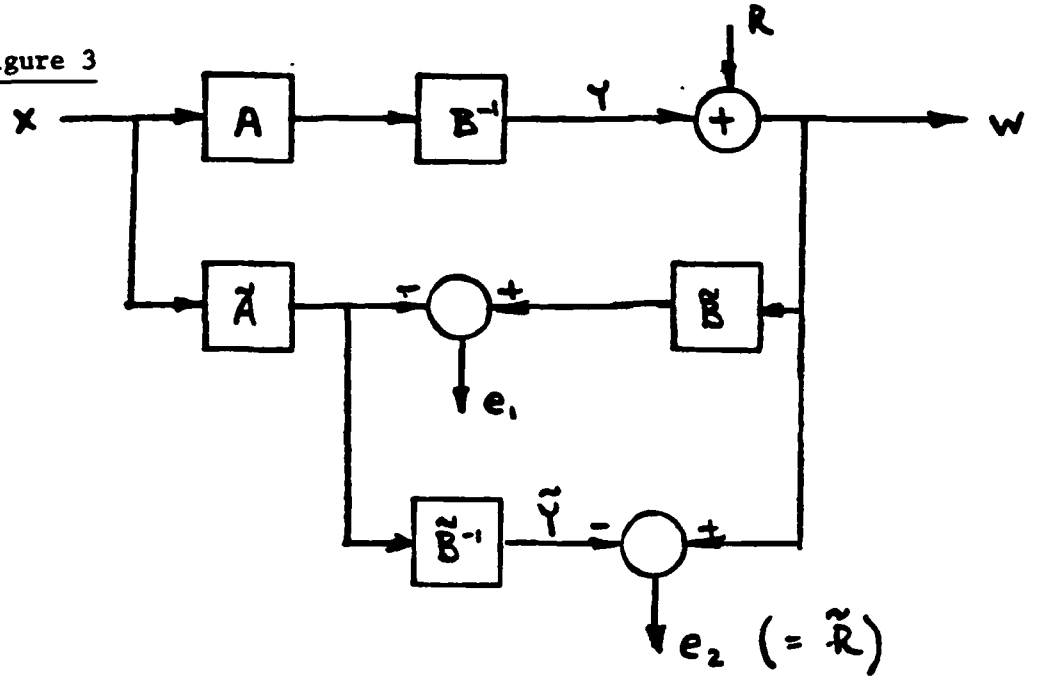

Figure 4

N denotes nonlinearity.

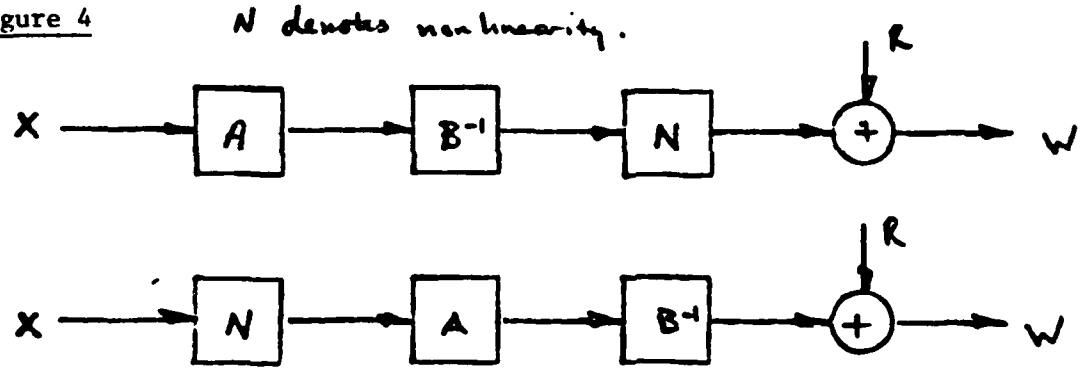

Appendix Least squared error and instrumental variables.

Given a system in which noise-free outputs are observable, the system, its input and output, can be represented as

$$S^T(\tilde{C} + \Delta C) = Y^T \tag{1}$$

where S, $\tilde{C}$, ΔC, and Y are as defined in the text.

If more measurements are made than the order of the system, then it is a case of n unknowns with n + m equations. If the system is perfect, this produces no problem. But any imperfections in measurement or in the system will produce results which are inconsistant, and the above equation for ΔC will be unsolvable. To remedy this, as error vector is defined to allow for the inconsistancies

$$E = S^T(\Delta C) - (Y^T - S^T\tilde{C}) \tag{2}$$

To arrive at the least squared error estimate, E^TE is minimized (with respect to ΔC):

$$\frac{\partial E^TE}{\partial \Delta C} = 0. \tag{3}$$

(In order to achieve a minimum.) In this case,

$$\frac{\partial E^TE}{\partial \Delta C} = 2\left(\frac{dE}{d(\Delta C)}\right)^T E \tag{4}$$

$$\frac{dE}{d(\Delta C)} = S^T, \tag{5}$$

and so

$$\frac{1}{2}\frac{\partial E^TE}{\partial(\Delta C)} = S(S^T(\Delta C) - (Y^T - S^T\tilde{C})). \tag{6}$$

Setting this equal to 0, and solving for ΔC,

$$\Delta C = (SS^T)^{-1}S(Y^T - S^T\tilde{C}). \tag{7}$$

This is the solution for a noise-free system.

The situation, however, is not noise-free, in that the observation W contains noise, and the signal matrix $\hat{S}$ as well. Putting these measurements into the calculation leads to a biased estimate of ΔC

$$\hat{S}^T(\Delta C) - \hat{S}^T(\Delta C) + S^T(\Delta C) = W^T - R^T - \hat{S}^T\tilde{C} + \hat{S}^T\tilde{C} - S^T\tilde{C} \tag{8}$$

Note that this equation is equivalent to (1).

Rewriting (8).

$$\hat{S}^T(\Delta C) = W^T - \hat{S}^T\tilde{C} + [(\hat{S}^T - S^T)(\Delta C) - R^T + (\hat{S}^T - S^T)\tilde{C}]$$

$$= W^T - \hat{S}^T\tilde{C} + [(\hat{S}^T - S^T)(\tilde{C} + \Delta C) - R^T] \qquad (9)$$

$[(\hat{S}^T - S^T)$ has terms dependent only on the noise vector, R, and $(\tilde{C} + \Delta C) = C$ is the true value of the coefficients for the proper (ΔC), and so the term in the brackets is dependent only on the noise and on the system - not the measurements or the estimate.]

Solving now for ΔC as if the measurements were noise free:

$$\Delta C = (\hat{S}\hat{S}^T)^{-1}\hat{S}(W^T - \hat{S}^T\tilde{C}) + \left\{(\hat{S}\hat{S}^T)^{-1}\hat{S}[(\hat{S}^T - S^T)C - R^T]\right\} \qquad (10)$$

But the computed value for ΔC would not include the term $\{\ \}$. Thus the bias of this estimate for ΔC is:

$$\text{BIAS} = E\left\{(\hat{S}\hat{S}^T)^{-1}\hat{S}[(\hat{S}^T - S^T)C - R^T]\right\} \neq 0 \qquad (11)$$

since the noisy signal vector correlates with the noise R. The technique of instrumental variables is similar to the above approach, but relies on an estimate of Y, $\tilde{Y}$ which is uncorrelated with the noise, R.

Now, using the estimated signal matrix $\tilde{S}$,

$$\Delta C = (\tilde{S}\hat{S}^T)^{-1}\tilde{S}(W^T - \hat{S}^T\tilde{C}) + \left\{(\tilde{S}\hat{S}^T)^{-1}\tilde{S}[(\hat{S}^T - S^T)C - R^T]\right\} \qquad (12)$$

where

$$E\left\{(\tilde{S}S^T)^{-1}\tilde{S}[(\hat{S}^T - S^T)C - R^T]\right\} = 0. \qquad (13)$$

The bias in the estimate is therefore removed.

END

FILMED

9-83

DTIC